copy 1

GUGGENHEIM AERONAUTICAL LABORATORY

CALIFORNIA INSTITUTE OF TECHNOLOGY

HYPERSONIC RESEARCH PROJECT

Memorandum No. 57
July 20, 1960

A STUDY OF AREA CHANGE NEAR THE DIAPHRAGM OF A SHOCK TUBE

by

David A. Russell

ARMY ORDNANCE CONTRACT NO. DA-04-495-Ord-1960

GUGGENHEIM AERONAUTICAL LABORATORY
CALIFORNIA INSTITUTE OF TECHNOLOGY
Pasadena, California

HYPERSONIC RESEARCH PROJECT

Memorandum No. 57

July 20, 1960

A STUDY OF AREA CHANGE NEAR THE DIAPHRAGM OF A SHOCK TUBE

by

David A. Russell

Clark B. Millikan, Director
Guggenheim Aeronautical Laboratory

ARMY ORDNANCE CONTRACT NO. DA-04-495-Ord-1960

ABSTRACT

The performance of a shock tube with area change near the diaphragm has been calculated for the high shock speed case by previous authors. This report extends the ideal theory calculations to include the whole shock speed range and all possible area changes near the diaphragm. Simple calculation procedures are presented and the practical applications of this type of area change are discussed.

Experimental measurements show excellent agreement with the theory except for the intermediate shock speed range where a non-steady secondary shock wave is predicted. Here not only is the agreement with the basic performance curves marginal, but detailed observations revealed that no secondary normal shock is present! A new model is devised to explain these discrepancies. This new model takes frictional effects into account and shows promise of being useful for other shock tube problems.

TABLE OF CONTENTS

LIST OF FIGURES

LIST OF SYMBOLS

a	speed of sound
A	cross-sectional area
A^*	throat cross-sectional area (M = 1)
A_s	cross-sectional area at shock position in nozzle (Appendix I. C)
g	amplification factor (Appendix I. A., Eq. 9)
g_s	amplification factor for shock-in-nozzle configuration (Appendix I. C)
M	Mach number
M_s	primary shock Mach number
P	static pressure
P_{Tg}	total pressure after probe normal shock wave
s	slope of fine wire response
t	ideal theory calculated time of arrival of event (measured from passage of primary shock wave)
	t_{cs} contact surface arrival
	t_{s2} secondary shock arrival
	t_e secondary expansion wave arrival
	t_{ee} end of secondary expansion wave
T	static temperature
u	velocity
u_{s2}	speed of secondary shock wave down the shock tube
x	distance along the shock tube (measured from the diaphragm station)
γ	ratio of specific heats
ρ	density

Subscripts

$( )_1$	parameter in region 1, the undisturbed driven gas
$( )_2$	parameter in region 2, downstream of contact surface
$( )_3$	parameter in region 3, upstream of contact surface
$( )_4$	parameter in region 4, the undisturbed driver gas

$( )_{3'}$, $( )_{3''}$, $( )_{4'}$ parameters in or adjacent to the area change (See Figure 1.)

$( )_a$ parameter in a general region a

$( )_b$ parameter in a general region b

I. INTRODUCTION

The types of cross-sectional area change that affect wave motion in a duct may be conveniently classified when boundary layer effects can be neglected. First there is the group in which, as a result of the area change, accelerating or decelerating waves are an essential feature of the flow (i. e., a long tapered tube), and second, the group for which all waves may be treated as having no acceleration. This classification is based on the relative length of time that the wave system spends in the region of varying area; the first group corresponds to the case where the wave system never emerges from the region of varying area, while in the second group the wave system has long since passed through the area change.

The configurations involving no wave acceleration have similarity solutions in the x-t plane about some origin. They may be divided into those configurations for which there are waves entering as well as leaving this origin (i. e., problems involving wave reflection[1])*, and those for which there are only waves leaving the similarity origin. For a shock tube the latter group is referred to as having area change "near the diaphragm". This implies that, for flow times of interest, the various waves have attained a state of constant velocity, wave reflection has ceased to be important, and the contact surface has passed through the region of varying area. The purpose of this report is to study this type of area change in a shock tube.

Shock tubes with area change near the diaphragm may be treated in ideal theory (Cf. Section II.) as though the area change were an isentropic nozzle located at the diaphragm. The calculation of shock tube performance is then basically a problem of matching pressure and velocity across the contact surface. In general, an upstream-facing secondary wave, between the nozzle exit and the contact surface, will be found necessary in order to achieve the contact surface matching. (Cf. Figure 1) For very high shock Mach numbers, this wave will be a non-steady expansion wave; for lower Mach numbers, a non-steady normal shock

---

* Superscripts denote references at the end of the text.

wave is required; for still lower Mach numbers, the normal shock wave moves into the nozzle and becomes stationary; while at the very low Mach numbers, the nozzle flow becomes subsonic, and thus incapable of supporting any secondary wave.

The above wave configurations are the only possible ones for a shock tube with area change near the diaphragm; however, a given shock tube may not produce them all. Previous work, notably by Resler, Lin, and Kantrowitz[2] and by Alpher and White[3]*, has been concerned with the use of area change at the diaphragm for the attainment of high speed shocks, and thus has only partially considered the first configuration (the case where the secondary wave is isentropic). In this report, the existing work is extended to all four configurations, and thus covers the whole range of shock Mach numbers and possible area changes at the diaphragm.

The ideal theory for the different configurations is discussed in the first section of the report. (Detailed calculation procedures are presented in Appendix I.) Curves of range of application and of initial pressure ratio versus shock Mach number are presented for Nitrogen-Air and Helium-Air shock tubes. The second section discusses the usefulness of various area configurations with the aid of the ideal theory. Particular attention is given to the use of a simple drilled plate inserted at the diaphragm, as a means of gaining additional flexibility in shock tube operation.

The agreement between experimental and theoretical curves of initial pressure ratio versus shock Mach number is discussed in the next section, where the fine wire and piezo-electric pressure gauge observations of the secondary waves are shown to indicate the necessity for a new model for the non-steady, non-isentropic configuration.

A simple model, based on the concept of the Fanno process, or spread out compression region, is presented in the fourth section. With this new theory the remarkable agreement with experimental basic performance is shown, and the insensitivity of the basic performance curves to the type of model is demonstrated. The inadequacies of this new theory are discussed, and more realistic models are indicated.

---

* Reference 3 includes a critical review of earlier work, and in particular points out an error in a previous study of the expansion wave configuration made at this laboratory. (Yoler, Y. A.: Hypersonic Shock Tube. GALCIT Hypersonic Research Project, Memorandum No. 18, July 19, 1954.)

II. IDEAL THEORY

The ideal theory is based on the assumptions of no heat transfer and no boundary layers or associated viscous interaction regions. These restrictive assumptions, which allow the use of isentropic nozzles and simple plane waves, will turn out to be remarkably good for predicting most of the performance characteristics of shock tubes with area change near the diaphragm. The procedure is based on matching conditions across the contact surface, and is set up so as to avoid the iterative calculations that are common to this type of problem.

The shock tube configurations studied are illustrated in Figure 1. Each model shown in similar to a plain shock tube, except for the changing area at the diaphragm station and the resultant secondary waves. The notation used is adapted from the accepted shock tube notation, where region 1 refers to the undisturbed driven gas, regions 2 and 3 to the gas downstream and upstream of the contact surface, and region 4 to the undisturbed driver gas. The primed numbers refer to the gas immediately upstream and downstream of the area change as shown. It should be noted that the secondary waves are always upstream of the contact surface, and are always upstream facing waves (although nonsteady waves are swept downstream by the flow). It can be shown that any other secondary wave configuration is unstable, for the wave will either tend to change its position to correspond to one of the configurations in Figure 1, or it will catch up with one of the primary waves.

The assumption that the area change may be treated as an isentropic nozzle enables the shock tube geometry to be completely specified by A_4/A_1 (the ratio of driver to driven tube area) and A^*/A_1 (the ratio of the throat area to the driven tube area). For a given shock tube with specified gases (i.e., a_4, γ_4, a_1, γ_1), the velocity downstream of the contact surface is uniquely determined by M_s (the shock Mach number), while the velocity upstream of the contact surface is fixed by the nozzle geometry (if the nozzle exit flow is assumed supersonic). Thus, there is only one value of M_s for which the velocity will match across the contact surface. For shock speeds above this value a second expansion wave is necessary to further expand the nozzle exit flow. This is the "expansion wave configuration" depicted in Figure 1a . For shock speeds below the

critical value, a normal shock wave will, in general, be expected (Figure 1b). As mentioned in the Introduction, this wave increases in strength as M_s is lowered, until it becomes stationary in the nozzle ... the "shock-in-nozzle" configuration (Figure 1c). Finally, for very low shock speeds, the nozzle flow becomes completely subsonic and no secondary waves can exist. Curves illustrating the regions of application of these various configurations are presented in Figure 2. for $A_4/A_1 = 1$.

The actual analyses are worked out in Appendix I. The ideal theory for the expansion wave configuration has been previously demonstrated for $A_4/A_1 > 1$ and $A^*/A_1 = 1$ (References 2 and 3)*, but is reviewed both as a background for the other configurations, and to show its logical extension to all values of A_4/A_1 and A^*/A_1. It is seen that the solution of the basic shock tube relation is available in closed form for this case. Indeed, an "equivalent standard shock tube" may be defined as shown in Appendix I. A. In this analysis it is not necessary to consider the speed of the secondary expansion wave itself, for the ratio of the parameters across the wave depends only on the flow Mach numbers on either side. For the normal shock wave configuration, however, the expression for the pressure ratio across the secondary shock involves the speed of the shock wave, and elimination of this speed in terms of the flow Mach numbers involves the solution of a high degree algebraic equation. The resulting calculation becomes so unwieldy that the usefulness of a closed form solution for the normal shock case is questionable. The procedure presented provides a relatively fast means of calculating performance, avoiding the necessity for iteration by not attempting to solve the direct problem in which M_s is specified. The shock-in-nozzle configuration is an extension of the shock wave case, simplified because the shock is stationary, but complicated because of the additional steady expansion.

Illustrative performance curves are shown in Figures 3 and 4 for the high M_s regions. These curves are for varying A^*/A_1 only. Figures 5a and 5b allow determination of the performance of a Helium-Air shock tube of any geometry, but for the expansion wave case only. Figure 12 shows the low M_s solution for a Nitrogen-Air shock tube again

---

* Reference 3 also considers the energy aspects of the problem ... considerations of energy transfer efficiency across the various wave systems affords a useful qualitative understanding of the whole process.

with varying A^*/A_1 only. Since the effect of the nozzle depends solely on A_4/A_1 for the "subsonic nozzle" configuration, that part of the curves of Figure 12 corresponds to the conventional shock tube curve.

The dividing line between the regions of application of the expansion wave and shock wave model does not readily come out of the expansion wave theory. It is arrived at by taking the limit of the normal shock wave theory, that is, where the secondary shock has zero strength

$$\left(M_{3'} - \frac{u_{s2}}{a_{3'}} = 1\right) .$$

The lower limit for the normal shock model is where the shock first becomes stationary ($u_{s2} = 0$); the lower limit for the shock in nozzle theory is where the shock is at the throat and has zero strength. These boundaries are depicted in Figure 2 for shock tubes with varying A^*/A_1.

III. APPLICATION OF AREA CHANGE AT THE DIAPHRAGM

One of the first studies of area change at the diaphragm was that of Lukasiewicz[4]. Both he and subsequent authors[2,3] have been primarily concerned with the interesting fact that area change may be used to increase available shock speed for a given shock tube. This effect is a maximum for $A^*/A_1 = 1$ and $A_4/A_1 \longrightarrow \infty$; however, from Figures 5a and 5b it is seen that a small increase in A_4 produces very nearly the same effect as the limit of infinitely large A_4/A_1. The actual per cent increase in M_s over that of a conventional shock tube is a complicated function of M_s itself, but Figures 5a and 5b illustrate it to be of the order of ten per cent for a practical shock tube operating at near maximum pressure ratio. Information contained in Reference 3 shows that this figure is reasonable for shock tubes operating with other gas combinations. While the figure of ten per cent is appreciable in some instances, other techniques will generally produce more spectacular increases (i.e., different gas combinations, a heated driver, or a double diaphragm shock tube[5]).

A study was made of the use of area change at the diaphragm for the economical operation of large shock tubes. The diaphragm cost (proportional to $A^{*3/2}$) turns out to be negligible when compared with that of the driver gas at the high pressure ratios where cost becomes significant. The gas volume is proportional to P_4A_4 , and it is readily shown that A^*/A_1 must be unity for optimum economy at a given M_s . The optimum value of A_4/A_1 , however, is not obvious, and curves of A_4/A_1 versus P_4A_4 must be plotted for each value of M_s. Such curves are presented in Figure 6. It is seen that the value of A_4/A_1 at which P_4A_4 is a minimum is a function of M_s as expected. The trend to higher optimum values of A_4/A_1 with increasing M_s is a result of the asymptotic behavior of the basic performance curves, such that the high values of M_s cannot reasonably be achieved in a plain shock tube where the M_s asymptote is low. For operation at moderate M_s it is seen from Figure 6 that a conventional shock tube ($A_4/A_1 = 1$) is not far off optimum for economical operation. For operation at high M_s , however, the above logic shows that the use of $A_4/A_1 > 1$ is most efficient, and Figure 6 illustrates that factors of ten or greater decrease in operating cost can be realized for a Helium-Air shock tube. Studies of this nature aide in the choice of

driver size, and they may result in a significant decrease in operating cost for a large shock tube.

The use of area change can provide additional flexibility in shock tube operation. Since the nozzle used in the ideal theory has no characteristic axial length, it may be assumed to have negligible length and to consist merely of a drilled plate placed perpendicular to the flow at the diaphragm station. Separation losses and consequent violation of the assumptions inherent in the ideal theory might now be expected, however the experimental evidence presented in the next section shows these losses to be negligible. Thus the use of a simple insert in a conventional shock tube enables any reduced area diaphragm shock tube to be easily obtained. The insert plates provide an additional control on Reynolds number, and they are a logical way to produce low shock speeds.*

Figures 3, 4, and 12 show the performance of such a modified shock tube; Figure 7 shows the diaphragm insert section used for obtaining the experimental results presented in this report. Placement of the drilled plate just far enough downstream to clear the opening diaphragm provides model and instrument protection from possible diaphragm fragments, and circumvents the rippage and uncertain breaking pressure problems associated with the alternative use of very thin diaphragms. For large shock tubes it may be desirable to reduce the diaphragm size and thickness, and this may be facilitated by clamping the diaphragm directly over the plate orifice.

---

* In addition, the ideal theory for the normal shock wave configuration predicts a jump in pressure after the primary shock wave, and a jump back to essentially the initial pressure after the passage of the secondary wave. This pressure pulse might have useful application, but the experimental evidence indicates that it is not to be expected for small shock tubes operating at reasonable pressure levels.

IV. EXPERIMENTAL RESULTS

An experimental study of area change near the diaphragm of a shock tube was undertaken in the GALCIT 3 inch square tube. The purpose of this study was to check the validity of the ideal theory, both by observing the basic performance of a modified shock tube, and by an investigation of the secondary waves. This shock tube has an area ratio of $A_4/A_1 = 0.855$, and was modified by the diaphragm insert of Figure 7. Nitrogen-Air runs were made with various insert plates giving a range of A^*/A_1 from 0.855 to 0.03. Varying the initial pressure from 5 - 500 mm. gave enough range in M_s to enable measurements to be made in all of the flow regimes involving secondary waves. A description of the shock tube and instrumentation used is presented in Appendix II.

The ideal theory predicts initial pressure ratio as a function of M_s with no attenuation. In order to experimentally verify these curves with M_s measured some distance down the tube, the attenuation must be taken into account. Thus, for the initial measurements, M_s was obtained at two stations spaced a maximum distance apart along the shock tube.

The resulting values of per cent attenuation per foot showed considerable scatter, and only order of magnitude correlation with theory[6]. This was presumably due to the uncertain effect of diaphragm opening time, and the relatively short distance over which it was possible to make the measurements. The measurements did show, however, that for a given M_s there is no consistent or appreciable dependence of attenuation on A^*/A_1. This means that a value of M_s, measured in a modified shock tube, may be corrected for attenuation by adding to it the difference between the ideal and the best fit experimental curves for the unmodified shock tube with the same M_s. Figure 8 presents the original P_4/P_1 versus M_s data. (Note that the ideal theory curves are plotted for $A_4/A_1 = 0.855$ and thus differ from those of Figure 12.) Figure 9 shows the data replotted with the small attenuation correction applied. The experimental points were obtained on different days and are accurate to the order of the symbol size. A few points, for which the diaphragms were only partially opened, fell understandably low and have been omitted.

The agreement between the theory and the corrected experimental results is seen to be excellent for the shock-in-nozzle configuration. The

experimental points also appear to fair into the ideal theory curve for the expansion wave case. The validity of the ideal theory for the expansion wave configuration was also noted by Alpher and White[7], who made measurements at high M_s in a shock tube with various values of A_4/A_1 and observed that the change in basic performance agrees with the theory. These results emphasize the general validity of the ideal theory and they imply that any nozzle plate losses are insignificant (from the standpoint of the ideal theory). Indeed, nozzle losses could be easily added into the theory (if the experimental data were available), but it is felt that the remaining uncertainties in attenuation are of more significance.

The discrepancy between theory and experiment for the normal shock configuration remains unexplained. In order to shed more light on this situation the actual details of the secondary waves were investigated for the normal shock wave and expansion wave configurations. The primary tool for this investigation was the fine unheated wire[8], for which the analysis techniques are discussed in Appendix II. Tungsten wires with diameters ranging from 1.5 - 0.2 mils. were used, affording a wide range of sensitivity. The wire response was expected to exhibit a sharp change in slope when a secondary shock wave passes over it, or a gradual change of slope through an expansion wave. The slope on each side of the secondary wave, together with the expected time of arrival of the wave at the gauge, was calculated and compared with the experimental results. The use of slope ratios eliminates some of the wire calibration properties, and it is felt that the resulting slope predictions are accurate to within ten per cent. Principle errors in this calculation are due to end losses, the cumbersome calculation procedure, and the extension of existing hot wire data to the current situation.

Typical results are presented in Figure 10, where the relevant theoretical and experimental slope ratios are also listed. Figure 10a, for the expansion wave regime, shows reasonable agreement, both in times and slope ratios. The normal shock wave results, however, did not show the expected change in slope. Indeed, there was no definite slope change observed for this configuration with any of the wires tested, and the predicted slope ratio was always considerably different from the observed value, indicating that the secondary normal shock model is incorrect.

An examination of the slope ratios for the normal shock configuration revealed that the experimental slope is always nearer to the predicted values of $s_2/s_{3'}$ than it is to s_2/s_3. Since no change in slope occurs after the contact surface, this might indicate that the secondary shock occurred at the contact surface. To check this unlikely possibility, and to provide additional information concerning this configuration, static pressure measurements were made using a commercially available crystal transducer. (Kistler Piezo-Calibrator Model 2 with S. L. M. pickup) A sample trace is shown in Figure 11a. These traces did not show the expected sharp pressure drop through the secondary shock wave. Instead, they showed the gradual pressure rise that has been observed in conventional shock tubes.[14]

It is unlikely that the shock wave is masked out at the wall by boundary layer inter-action, but total pressure measurements were made to check this possibility. A small total pressure probe was constructed, using a Barium Titanite crystal modeled after that of Reference 9. A trace from this instrument is shown in Figure 11b. There is a suggestion of a drop in total pressure, but it is not conclusive in that it is unfortunately obscured by hash from the diaphragm and a natural frequency of the crystal mounting. Since the total pitot pressure is relatively insensitive to the existence of a secondary normal shock, this study was not pursued further than a few unsuccessful attempts to clean up the response. It is felt that the measurements tended to support the previous findings of no secondary normal shock wave.

A final experimental study was made with a four inch wooden nozzle attached to the downstream side of the 0.03 inch orifice plate. The purpose of this nozzle was to check the effect of the plate itself on the existence of the normal shock wave. Fine wire results were essentially identical with and without the nozzle on the plate. The points on the P_4/P_1 versus M_s curves of Figures 8 and 9 fall a little high, but the results are too few to be conclusive, and are probably due to a change in the attenuation history. A smoothly contoured nozzle appears to produce the same shock tube flow as the orifice plates.

V. FRICTIONAL THEORY FOR THE NON-ISENTROPIC SECONDARY WAVE CONFIGURATIONS

The experimental results of the last section indicate that the normal shock model is marginal for predicting M_s and thus conditions in region 2, and quite inadequate for describing the flow details upstream of the contact surface. To agree with the measurements, a new theory for this non-isentropic configuration is needed which will predict no static pressure jump and no sharp slope changes in the fine wire response. The new theory must, in addition, predict nearly the same basic performance as the ideal theory, and must fair logically into the valid solutions for the other configurations.

The starting point for the new theory might logically be to consider the secondary shock to be replaced by many weak shocks, resulting in a spread out compression region. The existence of a spread out compression region in a supersonic duct has been studied in connection with wind tunnel nozzles[10, 11]. Indeed, in Reference 11 it is pointed out that the shock wave reflecting off the end of a shock tube has been observed to take this form. It would seem quite possible that the interaction between the secondary shock wave and the thick boundary layer from the diaphragm could also result in a spread out region for the configuration under study.

Appendix III. A. shows the relevant calculations for a new model based on the replacement of the secondary shock wave with such a stationary interaction region. The functional relationship of the flow variables across this region is that of a Fanno curve, and the model will be referred to as the Fanno process model. The relationship is obtained by writing the energy and continuity equations for the average cross-sectional flow values, replacing the momentum equation by a statement of the overall pressure ratio. This allows for arbitrary frictional processes and still enables the shock tube performance to be calculated, although the details in the Fanno region itself remain arbitrary. It should be mentioned that in the calculations that lead to the Fanno model, the exit Mach numbers may come out to be subsonic. Since a frictional process in a constant area duct cannot result in a transition from supersonic to subsonic flow[12], a stationary shock wave must exist within the Fanno regions for these cases.

Figure 12 shows the results of the Fanno process model for $A_4/A_1 = 1$.* Figure 9 shows the remarkable agreement between this model and the experimental data. It is seen that the new curves fair in with both the expansion wave and subsonic nozzle solutions, even though they may cross the ideal theory curve before doing so. It is interesting to note that there is no slope discontinuity corresponding to that which occurs at the junction of the normal shock and shock-in-nozzle solutions, and that the shock-in-nozzle solution itself is unchanged by the new theory.

An attempt was made to choose a combination of shock tube gases so as to further separate the two solutions and thus experimentally check the validity of the Fanno model under more severe conditions, but the relative M_s difference was quite insensitive to the gases used. The insensitivity of the basic performance to the model used is further exemplified by the fact that solutions which consist of part stationary Fanno process and part drifting secondary normal shock lie in the small enclosed region between the two pure solutions.

The agreement with the detailed flow measurements is also improved with the Fanno model. The calculated fine wire slope ratio for Figure 10b is -5.4 as compared with an experimental value of -7.7, and an ideal theory value of -2.0. The static pressure is now expected to remain constant, and while it actually tends to rise, this feature has been observed in plain shock tubes[14] and is thus not directly connected with the area change.

There is another interesting reason for accepting the Fanno model. From Reference 13 it can be inferred that the nozzle starting process is important for times as short as those involved in shock tube operation, and, in fact, the nozzle may not attain fully developed supersonic flow before the end of the run. A quasi-steady model of this situation might be to consider isentropic flow to a given station in the nozzle exit, and a Fanno process through the remainder of the nozzle. As time proceeds, more and more of the nozzle will be occupied with the isentropic flow and the Fanno region will move out of the nozzle. It is shown in Appendix III. B that for this model the flow parameters downstream of the Fanno process are independent of the location of the beginning of the Fanno process in the nozzle, and depend only on the overall pressure ratio across the whole

---

* The plain shock tube curve was obtained with the use of a Fanno process from sonic velocity, replacing that part of the driver expansion wave which was downstream of the diaphragm.

region. Thus this quasi-stationary model must give results identical with the previous Fanno curve model, a fact which lends further credence to that model.

The simple stationary Fanno model has shown appreciably better agreement with experiment than the ideal theory model, indeed the remaining unexplained differences are of the same nature as those which have been observed in a plain shock tube[14]. The use of the basic Fanno process idea, inter-related with a time-dependent mechanism for attenuation, may be a key to more complete understanding of these flows. The Fanno region may be combined with non-steady waves, may be allowed to drift down the tube, or may be assumed to grow with time (i. e., the downstream boundary moving with the speed of the contact surface). In the latter case, the time dependent equations may be simplified by the introduction of a conical flow parameter, but the detailed history of one variable is needed to replace the momentum equation, and solution difficulties arise for all but the most simple assumed profiles.

A model, consisting of a stationary Fanno curve with a weak expansion wave downstream, was tried in an attempt to explain the wall pressure rise with time that existed for all shock tube configurations. Some agreement with experiment was obtained, but more detailed measurements are necessary in order to justify the existence of this type of model, and to provide a thorough understanding of the Fanno-type of frictional process in a shock tube. In particular, it would be useful to learn more of when this process may be advantageously used in place of the more complicated boundary layer approaches.

VI. CONCLUSIONS

1. The ideal theory presented in this report accurately predicts M_s for shock tubes with area change near the diaphragm, with the exception of those configurations where a moving secondary shock wave is expected.

2. In cases involving moving secondary shock waves, the stationary Fanno curve model discussed in this report accurately predicts M_s and provides agreement with flow details to the same degree that flow measurements agree with theory for a plain shock tube. Further refinement of the theory, to coincide more closely with observation, awaits a more detailed experimental investigation. It is suggested that the Fanno-type of frictional process might have useful application to other shock tube problems.

3. It appears that the most practical applications of area change at the diaphragm are the use of A_4/A_1 for increased M_s, and the use of simple insert plates to provide an additional control on shock tube performance. In addition to these, and certain advantages that may occur in large shock tubes, area change near the diaphragm offers an interesting research tool for a further understanding of shock tube flows.

REFERENCES

1. Monroe, L. L.: "Investigation of the Transmission of a Shock Wave through an Orifice". GALCIT Hypersonic Research Project, Memorandum No. 46, September 25, 1958.

2. Resler, E. L.; S. C. Lin; A. Kantrowitz: "The Production of High Temperature Gases in Shcok Tubes". J. Appl. Phys., 23, 1390, (1952).

3. Alpher, R. A.; D. R. White: "Ideal Theory of Shock Tubes with Area Change Near Diaphragm". General Elecgric Research Laboratory Report No. 57-RL-1664, January, 1957.

4. Lukasiewicz, J.: "Shock Tube Theory and Application". National Aeronautical Establishment Report No. 15, Ottawa, Canada, (1952).

5. Hall, J. G.: "Shock Tubes". Institute of Aerophysics, University of Toronto, UTIA Review No. 12, Part II, May, 1958.

6. Mirels, H.: "Attenuation in a Shock Tube Due to Unsteady-Boundary-Layer Action". NACA TN 3278, August, 1956. (See also, TN 4021).

7. Alpher, R. A.; D. R. White: "Flow in Shock Tubes with Area Change at the Diaphragm Section". J. Fluid Mech., 3, pp. 457-470, February, 1958.

8. Christiansen, Walter H.: "Use of Fine Unheated Wires for Heat Transfer Measurements in the Shock Tubes". GALCIT Hypersonic Research Project, Memorandum No. 55, June 1, 1960.

9. Willmarth, W. W.: "Small Barium Titanate Transducer for Aerodynamic or Acoustic Pressure Measurements". Rev. of Sci. Instruments, Vol. 29, No. 3, pp. 218-222, March, 1958.

10. Emmons, H. W.: "Fundamentals of Gas Dynamics". Princeton High Speed Aerodynamics and Jet Propulsion Series, Vol. 3, Princeton University Press, 1958.

11. Lukasiewicz, J.: "Diffusers for Supersonic Wind Tunnels". J. Aeronautical Sci., 20, p. 618, (1953).

12. Liepmann, H. W.; A. E. Puckett: "Introduction to Aerodynamics of a Compressible Fluid". John Wiley and Sons, Inc., New York, N. Y., (1947).

13. Bull, G. V.: "Starting Processes in an Intermittant Supersonic Wind Tunnel". Institute of Aerophysics, University of Toronto, UTIA Report No. 12, February, 1951.

14. Emrich, R. J.; R. L. Peterson: "Pressure Variation with Time in the Shock Tube". Lehigh University Institute of Research T. R. 7, March 15, 1956. (See also TR 4, 5, and 8.)

15. Ames Research Staff: "Equations, Tables, and Charts for Compressible Flow". NACA Report 1135, 1953.

16. Mueller, J. N.: "Equations, Tables, and Figures for Use in the Analysis of Helium Flow at Supersonic and Hypersonic Speeds". NACA TN 4063, September, 1957.

17. Rabinowicz, J.: "Aerodynamic Studies in the Shock Tube". GALCIT Hypersonic Research Project, Memorandum No. 38, June 10, 1957.

18. Laufer, J.; R. McClellan: "Measurements of Heat Transfer from Fine Wire in Supersonic Flows". J. of Fluid Mech., Vol. 1, Part 3, p. 276, Sept., 1956.

19. Spangenberg, W. G.: "Heat-Loss Characteristics of Hot-Wire Anemometers at Various Densities in Transonic and Supersonic Flow". NACA TN 3381, May, 1955.

20. "Tables of Thermal Properties of Gases". National Bureau of Standards Circular 564, November 1, 1955.

APPENDIX I

IDEAL THEORY CALCULATION PROCEDURES

It may readily be shown from one-dimensional shock theory that

$$P_a/P_b = 1 + (2\gamma/\gamma + 1)(M_b^2 - 1) \quad , \tag{1}$$

transforming velocity so as to apply to a shock tube results in

$$P_2/P_1 = 1 + (2\gamma/\gamma+1)(M_s^2 - 1) \quad . \tag{2}$$

A similar procedure results in

$$u_2/a_1 = (2/\gamma_1+1)\left(M_s - \frac{1}{M_s}\right) \quad . \tag{3}$$

Hence,

$$u_2/a_1 = \left(\frac{P_2}{P_1} - 1\right)\left[\gamma_1 \frac{(\gamma_1+1)}{2}\left(\frac{P_2}{P_1} - 1\right) + \gamma_1^2\right]^{-\frac{1}{2}} . \tag{4}$$

The Riemann invariant applied across a non-steady isentropic wave results in:

$$P_a/P_b = \left[\rho_a/\rho_b\right]^{\gamma} = \left[a_a/a_b\right]^{2\gamma/\gamma-1} = \left[\frac{1 + \frac{\gamma-1}{2} M_b}{1 + \frac{\gamma-1}{2} M_a}\right]^{2\gamma/\gamma-1} , \tag{5}$$

while the energy relation applied across a steady isentropic process results in

$$P_a/P_b = \left[\rho_a/\rho_b\right]^{\gamma} = \left[a_a/a_b\right]^{2\gamma/\gamma-1} = \left[\frac{1 + \frac{\gamma-1}{2} M_b^2}{1 + \frac{\gamma-1}{2} M_a^2}\right]^{\gamma/\gamma-1} . \tag{6}$$

In the following analyses, extensive use is made of the tables for the parameter relationships across a stationary normal shock wave, and tables for steady isentropic flow with area change[15, 16]. The calculations are arranged so that only these tables and curves of Eq. (4) need be obtained in order to calculate the complete performance of a given shock tube. In the following calculations, perfect gases have been assumed throughout.

A. Expansion Wave Configuration

Referring to Figure 1a, the overall pressure ratio may be written as

$$P_4/P_1 = (P_4/P_{4'})(P_{4'}/P_{3'})(P_{3'}/P_3)(P_3/P_2)(P_2/P_1) \quad . \qquad (7)$$

Applying Eq. (5) across the non-steady expansion waves (regions 4-4' and 3'-3), Eq. (6) through the supersonic nozzle (4'-3'), and applying the pressure boundary condition, $P_3 = P_2$, yields:

$$(P_4/P_1) = \left[1 + \frac{\gamma_4-1}{2} M_{4'}\right]^{(2\gamma_4)/(\gamma_4-1)} \left[\frac{1 + \frac{\gamma_4-1}{2} M_{3'}^2}{1 + \frac{\gamma_4-1}{2} M_{4'}^2}\right]^{(\gamma_4)/(\gamma_4-1)}$$

$$\times \left[\frac{1 + \frac{\gamma_4-1}{2} M_3}{1 + \frac{\gamma_4-1}{2} M_{3'}}\right]^{(2\gamma_4)/(\gamma_4-1)} (P_2/P_1) \quad . \qquad (8)$$

Now, extending the results of Reference 2, define an "amplification factor":

$$g = \left[\frac{1 + \frac{\gamma_4-1}{2} M_{4'}^2}{1 + \frac{\gamma_4-1}{2} M_{3'}^2}\right]^{(\gamma_4)/(\gamma_4-1)} \left[\frac{1 + \frac{\gamma_4-1}{2} M_{3'}}{1 + \frac{\gamma_4-1}{2} M_{4'}}\right]^{(2\gamma_4)/(\gamma_4-1)} \qquad (9)$$

g is a constant, depending only on the driver gas and the parameters A_4/A_1 and A^*/A_1. It may readily be determined with the use of tables[15, 16]. Curves of g for all values of the area parameters are shown in Figure 5a for a Helium-Air shock tube. Since A_4/A_1 cannot be less than A^*/A_1 by definition, the line where these ratios are equal forms the left-hand boundary and each curve for a given value of A_4/A_1 must terminate on this boundary. Previous work[2, 3] has been concerned only with the case where $A^*/A_1 = 1$; inclusion of the effect of A^*/A_1 results in a complete surface as shown.

Equations (8) and (9) result in

$$P_4/P_1 = \frac{1}{g\left(\frac{A_4}{A_1}, \frac{A^*}{A_1}, \gamma_4\right)} \left[1 + \frac{\gamma_4 - 1}{2} M_3\right]^{(2\gamma_4)/(\gamma_4 - 1)} (P_2/P_1) \quad . \quad (10)$$

The velocity boundary condition, $u_2 = u_3$, enters through M_3:

$$M_3 = (u_3/a_3) = (u_2/a_3) = (u_2/a_1)(a_1/a_4)(a_4/a_{4'})(a_{4'}/a_{3'})(a_{3'}/a_3) \quad .$$

Using Eqs. (5), (6), and (9):

$$M_3 = (u_2/a_1)(a_1/a_4)\, g^{\frac{\gamma_4 - 1}{2\gamma_4}} \left(1 + \frac{\gamma_4 - 1}{2} M_3\right) \quad . \quad (12)$$

Solving Eq. (12) for M_3 and inserting into Eq. (10), there is obtained

$$P_4/P_1 = (1/g)(P_2/P_1) \left[1 - \frac{\gamma_4 - 1}{2} (u_2/a_1) \left(\frac{a_1}{a_4}\, g^{-(\gamma_4 - 1)/(2\gamma_4)}\right)\right]^{-(2\gamma_4)/(\gamma_4 - 1)} \quad (13)$$

Thus, assuming a given M_s, one may calculate u_2/a_1 and P_2/P_1 from relations 2 and 3. Knowing g, P_4/P_1 may be calculated, and in a similar manner any of the flow parameters arrived at.

Reference should be made to the well known connection between the above theory and that of a standard shock tube. The standard shock tube equation may be obtained by putting g = 1 in Eq. (13):

$$P_4/P_1 = P_2/P_1 \left[1 - \frac{\gamma_4 - 1}{2} (u_2/a_1)(a_1/a_4)\right]^{-(2\gamma_4)/(\gamma_4 - 1)} . \quad (14)$$

Comparing Eqs. (13) and (14), it is seen that the area-ratio tube produces the same shock speed for a given P_4/P_1 as a standard tube with the following modifications:

$$(a_1/a_4)_{\text{standard}} = g^{-(\gamma_4 - 1)/(2\gamma_4)} (a_1/a_4)_{\text{area ratio}} \quad (15)$$

$$(P_4/P_1)_{\text{standard}} = g\,(P_4/P_1)_{\text{area ratio}}$$

B. Normal Shock Wave Configuration

Starting as in the previous case, applying the pressure boundary condition and relations 5, 6, and 9, the overall pressure ratio becomes:

$$P_4/P_1 = (P_{3'}/P_3)(P_2/P_1) \quad \frac{\left[1 + \frac{\gamma_4 - 1}{2} M_{3'}\right]^{(2\gamma_4)/(\gamma_4-1)}}{g}$$

$$= C_1 \left(\frac{A_4}{A_1}, \frac{A^*}{A_1}, \gamma_4 \right) (P_{3'}/P_3)(P_2/P_1) \quad , \tag{16}$$

where the notation is that of Figure 1b.

The velocity boundary condition results in

$$u_2/a_1 = u_3/a_1 = (u_3/u_{3'})(u_{3'}/a_{3'})(a_{3'}/a_{4'})(a_4/a_1) \quad . \tag{17}$$

Again using Eqs. (5), (6), and (9):

$$u_2/a_1 = u_3/u_{3'} \left(\frac{a_4}{a_1} \frac{M_{3'}}{1 + \frac{\gamma_4 - 1}{2} M_{3'}} g^{(\gamma_4-1)/(2\gamma_4)} \right.$$

$$= C_2 \left(\frac{A_4}{A_1}, \frac{A^*}{A_1}, \gamma_4, \frac{a_4}{a_1} \right) (u_3/u_{3'}) \quad . \tag{18}$$

Now consider region 3 - 3' and define the secondary shock velocity as u_{s2}. Transforming to a stationary shock system, the flow Mach number into the shock becomes

$$\left(M_{3'} - \frac{u_{s2}}{a_{3'}}\right) .$$

Eq. (1) then yields:

$$P_3/P_{3'} = 1 + \frac{2\gamma_4}{\gamma_4 + 1} \left(\left[M_{3'} - \frac{u_{s2}}{a_{3'}} \right]^2 - 1 \right) \quad . \tag{19}$$

The calculation procedure is as follows:

(1) Assuming supersonic flow out of the nozzle, obtain $M_{3'} \left(\frac{A_4}{A_1}, \frac{A^*}{A_1}, \gamma_4 \right)$ from the tables and evaluate C_1 and C_2 in Eqs. (16) and (18).

(2) Now assume a value for $u_{s2}/a_{3'}$ and calculate $P_3/P_{3'}$ from Eq. (19). Knowing the flow Mach number into the shock $M_{3'} = (u_{s2}/a_{3'})$, calculate or obtain from the tables the exit flow Mach number $M_3 = (u_{s2}/a_3)$, and the speed of sound ratio $a_{3'}/a_3$.

(3) M_3 may be found from the relation:

$$M_3 = \text{exit flow Mach number} + \frac{u_{s2}}{a_{3'}} (a_{3'}/a_3) \quad . \tag{20}$$

The velocity ratio across the moving shock becomes:

$$u_3/u_{3'} = M_3/M_{3'} (a_3/a_{3'}) \quad . \tag{21}$$

(4) Knowing $u_3/u_{3'}$, Eq. (18) determines u_2/a_1, Eqs. (4) and (2) determine P_2/P_1 and M_s. It is suggested that the P_2/P_1 versus u_2/a_1 curves referred to at the beginning of the section be used to determine P_2/P_1, and M_s be either calculated from this value (Eq. 2) or picked out of the tables.

(5) With P_2/P_1 and $P_{3'}/P_3$ known, P_4/P_1 is readily calculated from Eq. (16).

C. Shock-In-Nozzle Configuration

The velocity of the secondary shock was initially assumed for the shock wave configuration analysis. In this case, however, the shock is stationary, and it is necessary to assume the shock position in the nozzle. Denoting the nozzle area at this position as A_s, the equation analogous to Eq. (16) is

$$P_4/P_1 = \left[(P_{3''}/P_{3'})(P_{3'}/P_3)\right] P_2/P_1 \quad \frac{\left[1 + \frac{\gamma_4 - 1}{2} M_{3''}\right]^{(2\gamma_4)/(\gamma_4 - 1)}}{g_s} \tag{22}$$

where $g_s = g\left(\frac{A_4}{A_s}, \frac{A^*}{A_s}\right)$ and the notation is in Figure 1c.

The velocity boundary condition yields:

$$u_2/a_1 = u_3/a_1 = M_3 (a_3/a_{3'})(a_{3'}/a_{3''})(a_{3''}/a_{4'})(a_{4'}/a_4)(a_4/a_1) \quad . \tag{23}$$

Applying Eqs. (5), (6), and (9):

$$u_2/a_1 = \left[M_3\,(a_3/a_{3'})(a_{3'}/a_{3''})\right]\,(a_4/a_1)\,\frac{g_s^{(\gamma_4-1)/(2\gamma_4)}}{1+\frac{\gamma_4-1}{2}\,M_{3''}}\,. \qquad (24)$$

The knowledge of A_4/A_s, A^*/A_s, and γ_4 enables g_s and $M_{3''}$ to be calculated[15, 16]. The shock tables and the value of $M_{3''}$ then give $P_{3''}/P_{3'}$, $a_{3'}/a_{3''}$, and $M_{3'}$. Allowing the subsonic flow at station 3' to expand, M_3, $P_{3'}/P_3$, and $a_3/a_{3'}$, can be obtained by using the tables and the value of $M_{3'}$ and A_s/A_1. Thus u_2/a_1 can be found from Eq. (24), and P_2/P_1 then obtained from the curves of Eq. (4). The value of P_2/P_1 and the shock tables yield M_s, and P_4/P_1 is determined from Eq. (22).

D. Subsonic Nozzle Configuration

In this case the nozzle flow is completely subsonic and conditions between regions 4' and 3 depend only on A_4/A_1. The performance may be calculated by the procedure of Appendix I. A, putting conditions in region 3' equal to those in region 3 (since no secondary expansion wave exists), and choosing the subsonic value for M_3. As expected, the resulting relations are identical with those for a plain shock tube when $A_4/A_1 = 1$, and there is an effect on performance only if $A_4/A_1 \neq 1$.

APPENDIX II

EXPERIMENTAL EQUIPMENT AND INSTRUMENTATION

The GALCIT three inch square shock tube was used for the experimental measurements. This is essentially the shock tube reported in Reference 17, but the pressure seals have been improved and the two-dimensional nozzle at the end of the tube has been replaced by a dump chamber. The shock tube has a circular driver such that $A_4/A_1 = 0.885$, and was modified for this series of tests by the diaphragm insert section of Figure 7. 0.006 inch aluminum diaphragms were used primarily. They were scored to break under a driver pressure from 20 - 100 psi. It was found that careful scoring resulted in the ability to repeat a given M_s to within 10 per cent. Some copper diaphragms were used, but it was found that the measured attenuation was not affected, and the basic performance virtually unchanged.

The shock speed was detected with two thin film platinum gauges spaced two feet apart, their average distance from the diaphragm being 16.7 feet. The gauges had high resistance (500 Ω) in order to maximize sensitivity for the low values of M_s. The output was fed through low noise level amplifiers to a Berkeley counter in the standard fashion. 10^{-2} A. current provided enough sensitivity to readily obtain shock speeds as low as $M_s = 1.04$. For the attenuation measurements, two pairs of gauges were used, the center of the second pair four feet upstream of the center of the first. Each pair was connected in series, fed through an amplifier, differentiated, and fed into the period function of a Berkeley counter.

The initial pressure was measured with a Wallace and Tiernan 0 - 50 mm gauge and an aircraft type manometer. The driver pressure was measured with a 0 - 100 psi. bourdon gauge. All gauges were carefully calibrated with either a McCleod gauge or known reference volumes, and the shock tube leak rate was maintained at a relatively low level.

The fine wires were constructed as in Reference 8. A constant excitation current was applied and the voltage across the wire was

directly sensed by an oscilloscope. The wire acts like a calorimeter, and thus its response to a given flow change is roughly exponential with time. Thus, for small times relative to the characteristic time, the slope of the wire response will be constant; for very long times, the wire response will be a step function. It was found that a wire chosen so as to have the former response characteristic was the most practical for these tests.

Given a specific M_s and P_1, all the flow variables could be calculated from the ideal theory. Approximate Nusselt numbers for the various flow regions could then be found from the calculated Reynolds and Mach numbers through the use of References 18 and 19. The Nusselt number is defined as

$$Nu = \frac{q\,d}{K\,(T_r - T_w)} \quad , \tag{1}$$

where d is the wire diameter, K the thermal conductivity of the fluid (evaluated at total temperature[20]), T_r the recovery temperature, and T_w the initial wire temperature. The heat transfer per unit area of wire, q, may be shown to be directly proportional to s, the response slope[8]. Thus,

$$s_2/s_3 = q_2/q_3 = \frac{K_2\,(T_{r_2} - T_1)}{K_3\,(T_{r_3} - \left[T_{r_1} + \Delta T_2\right])}\,(Nu_2/Nu_3) \quad . \tag{2}$$

It may also be shown that[8]

$$\Delta T_2 = \frac{\Delta E_2}{a_1\,I_w\,R_w} \quad , \tag{3}$$

where I_w is the wire current ($\approx 2(10)^{-3}$ A.), R_w the wire resistance at T_1 ($\approx 2\Omega$), a the coefficient of resistivity (taken as $0.004\,\Omega/^{\circ}C$ for tungsten), and ΔE the voltage jump on the experimental response trace. ΔT_2 was of the order of $50^{\circ}C$ for the $1\frac{1}{2}$ mil. wire.

Eq. (2) predicts the slope ratio between regions 2 and 3 when the recovery factors and Nusselt numbers have been found. The equation may easily be extended to other regions if care is taken in obtaining the wire temperature at the beginning of each change in slope.

APPENDIX III

THE FANNO PROCESS MODEL

A. Constant Area Fanno Model

In this study, the secondary normal shock of Figure 1b is replaced with a stationary compression region supported by shock boundary layer interaction. This interaction region is assumed to take place in the constant area duct, and, as in the ideal theory, the entering flow (region 3') is assumed known.

Assuming a perfect gas, the steady energy equation is

$$(a_a/a_b)^2 = \frac{1 + \frac{\gamma-1}{2} M_b^2}{1 + \frac{\gamma-1}{2} M_a^2} = (P_a/P_b)(\rho_b/\rho_a) \quad . \tag{1}$$

The continuity equation, applied between regions 3 and 3' may be written as:

$$(P_3 M_3)/a_3 = (P_{3'} M_{3'})/a_{3'} \quad , \tag{2}$$

where it is understood that flow parameters describing the Fanno region are the average values across the cross section.

Applying Eq. (1) across the Fanno region, and substituting $a_3/a_{3'}$ from Eq. (2) yields

$$(1 + \tfrac{\gamma-1}{2} M_{3'}^2) \left[\frac{P_{3'} M_{3'}}{P_3} \right]^2 = M_3^2 (1 + \tfrac{\gamma-1}{2} M_3^2) \quad . \tag{3}$$

Solving for M_3

$$(\gamma-1) M_3^2 = -1 + \left[1 + 2 (\gamma-1)(1 + \tfrac{\gamma-1}{2} M_{3'}^2) \left\{ (P_{3'}/P_3) M_{3'} \right\}^2 \right]^{\frac{1}{2}} . \tag{4}$$

The shock tube performance is readily calculated by first assuming $P_{3'}/P_3$. Then, since $M_{3'}$ is known, M_3 may be found. From this information $a_3/a_{3'}$ is obtained from Eq. (2). u_3/a_1 may now be determined, and the performance calculated in a manner analogous to that of Appendix I.

B. Varying Area Fanno Model

For this model, the Fanno process is assumed to take place in the nozzle itself. The flow is assumed to expand isentropically from the sonic throat to some station 3' and then proceed along a Fanno curve to a station downstream of the nozzle. (See sketch.) The entering flow is known, as well as A^*/A_3 , $A_{3'}/A_3$, and P_*/P_3 .

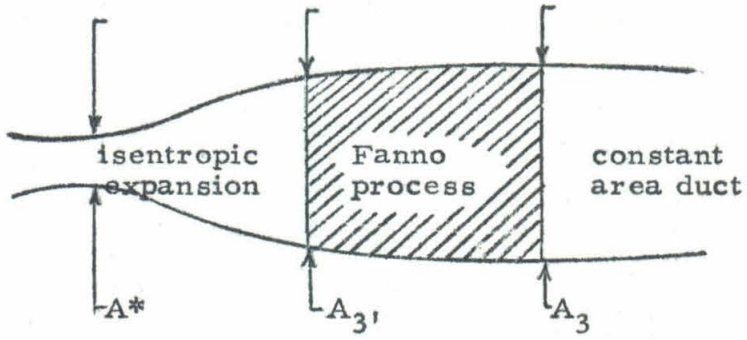

The isentropic relation between the throat and station 3' gives

$$P_*/P_{3'} = \left[\rho_*/\rho_{3'}\right]^{\gamma} = \left[a_*/a_{3'}\right]^{2\gamma/\gamma-1} \quad . \tag{5}$$

Appropriately applying Eqs. (1) and (5), the overall density ratio may be written:

$$\rho_*/\rho_3 = (\rho_*/\rho_{3'})(\rho_{3'}/\rho_3) = \left[\frac{1+\frac{\gamma-1}{2}M_{3'}^2}{(\gamma+1)/2}\right]^{1/\gamma-1}\left[\frac{1+\frac{\gamma-1}{2}M_{3'}^2}{1+\frac{\gamma-1}{2}M_3^2}\right]\frac{P_{3'}}{P_3}\,; \tag{6}$$

but

$$P_{3'}/P_3 = (P_{3'}/P_*)(P_*/P_3) = \left[\frac{(\gamma+1)/2}{1+\frac{\gamma-1}{2}M_{3'}^2}\right]^{\gamma/\gamma-1}(P_*/P_3) \quad . \tag{7}$$

Thus, collecting terms:

$$\rho_*/\rho_3 = \frac{(\gamma+1)/2}{1+\frac{\gamma-1}{2}M_3^2}\,(P_*/P_3) \quad , \tag{8}$$

and the continuity equation and perfect gas relation yield:

$$M_3 = (\rho_*/\rho_3)(a_*/a_3)(A_*/A_3) = \left[\rho_*/\rho_3\right]^{\frac{1}{2}} \left[P_*/P_3\right]^{\frac{1}{2}} (A_*/A_3) \quad . \qquad (9)$$

Applying Eq. (8) to Eq. (9) and solving the algebraic relation:

$$(\gamma - 1)\, M_3^{\,2} = -1 + \left[\, 1 + (\gamma^2 - 1) \left[(P_*/P_3)(A_*/A_3)\right]^2 \right]^{\frac{1}{2}} \quad ; \qquad (10)$$

but, again, applying continuity and Eq. (8):

$$u_3/a_* = (\rho_*/\rho_3)(A^*/A_3) = \frac{(\gamma+1)/2}{1 + \frac{\gamma-1}{2} M_3^{\,2}} (P_*/P_3)(A^*/A_3) \quad , \qquad (11)$$

and Eq. (11) together with Eq. (10)

$$u_3/a_* = \frac{(\gamma+1)\left[(P_*/P_3)(A^*/A_3)\right]}{1 + \left[1 + (\gamma^2 - 1)\left[(P_*/P_3)(A^*/A_3)\right]^2\right]^{\frac{1}{2}}} \quad . \qquad (12)$$

Eqs. (8), (10), and (12) demonstrate that the exit flow is independent of the position of station 3'. Thus the Fanno process could be completely outside of the nozzle, so that this solution is identical to that of part A above.

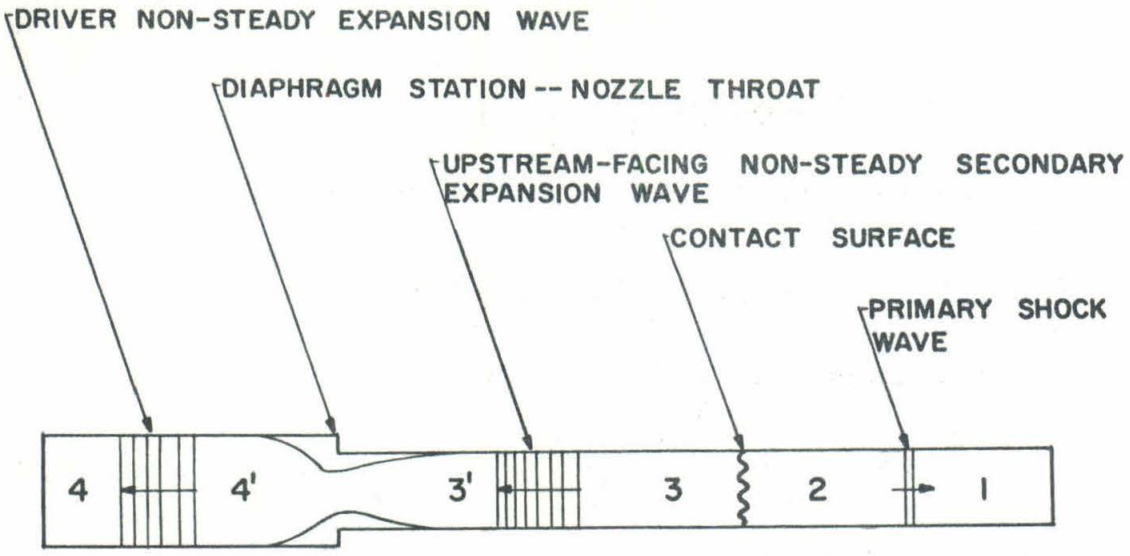

a. EXPANSION WAVE CONFIGURATION

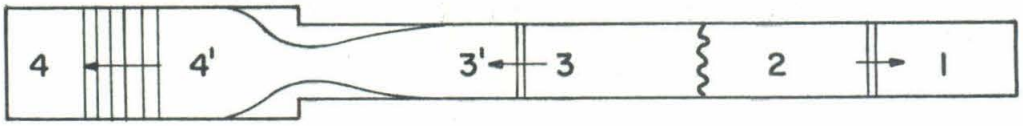

b. SHOCK WAVE CONFIGURATION

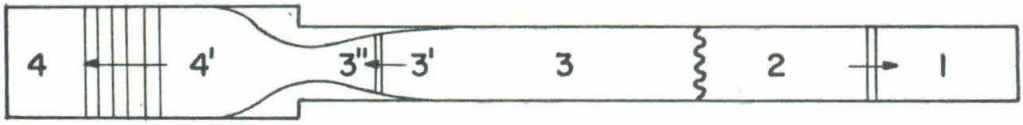

c. SHOCK-IN-NOZZLE CONFIGURATION

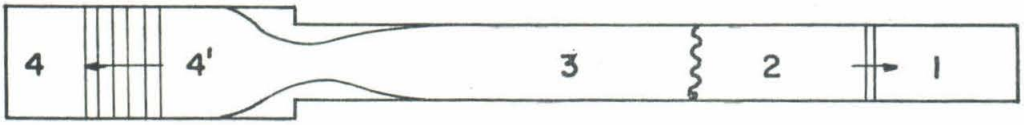

d. SUBSONIC NOZZLE CONFIGURATION

FIG. 1 SCHEMATIC SHOCK TUBE CONFIGURATIONS

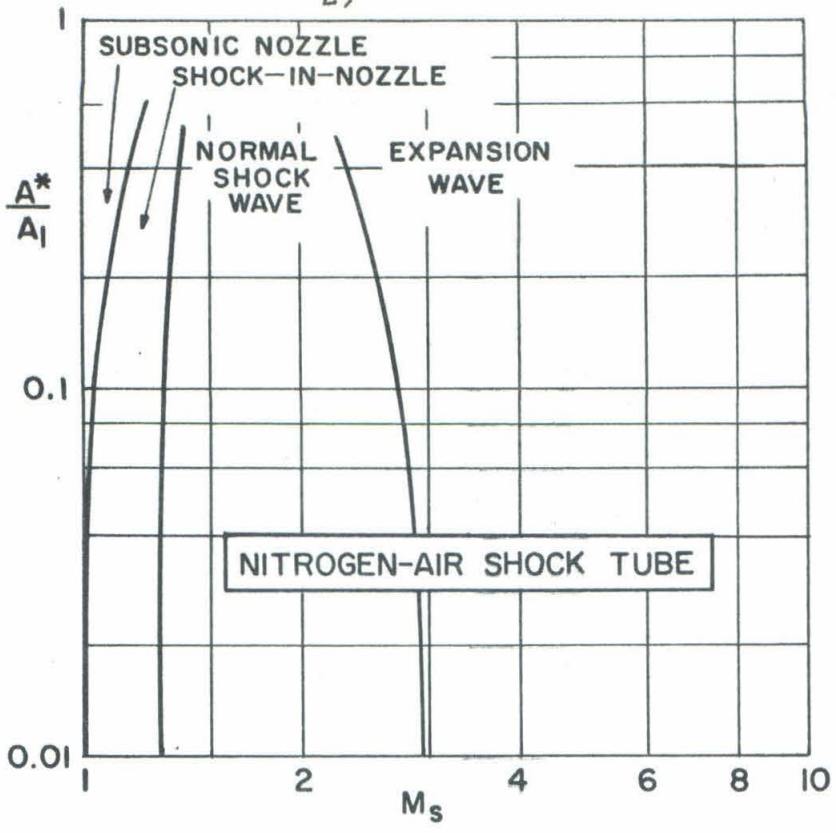

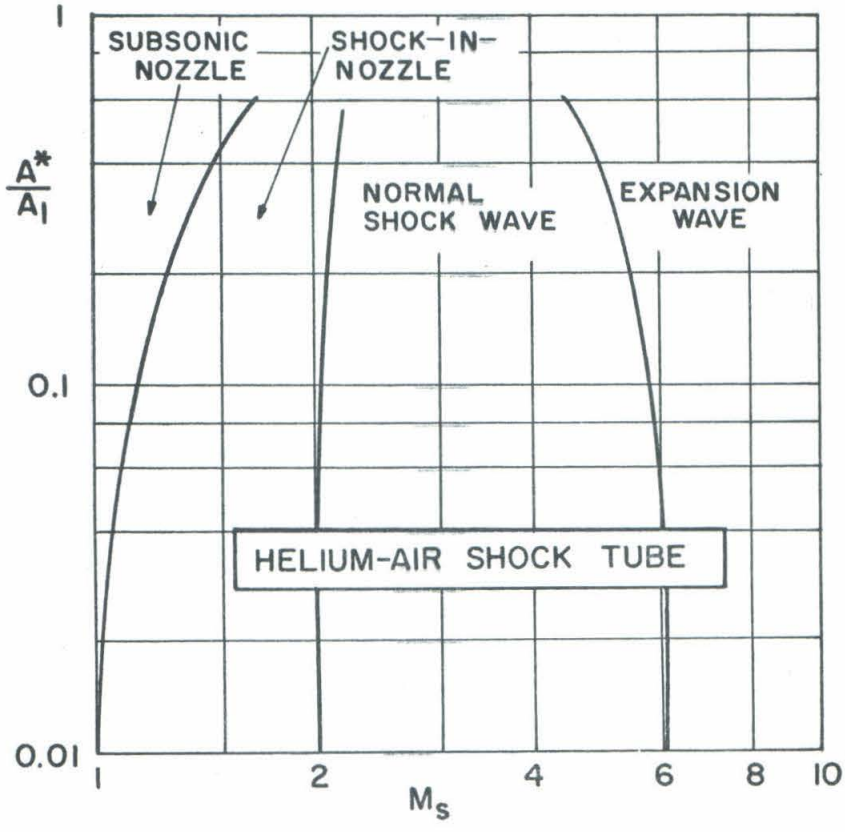

FIG. 2 CONFIGURATION BOUNDARIES FOR $A_4/A_1 = 1$

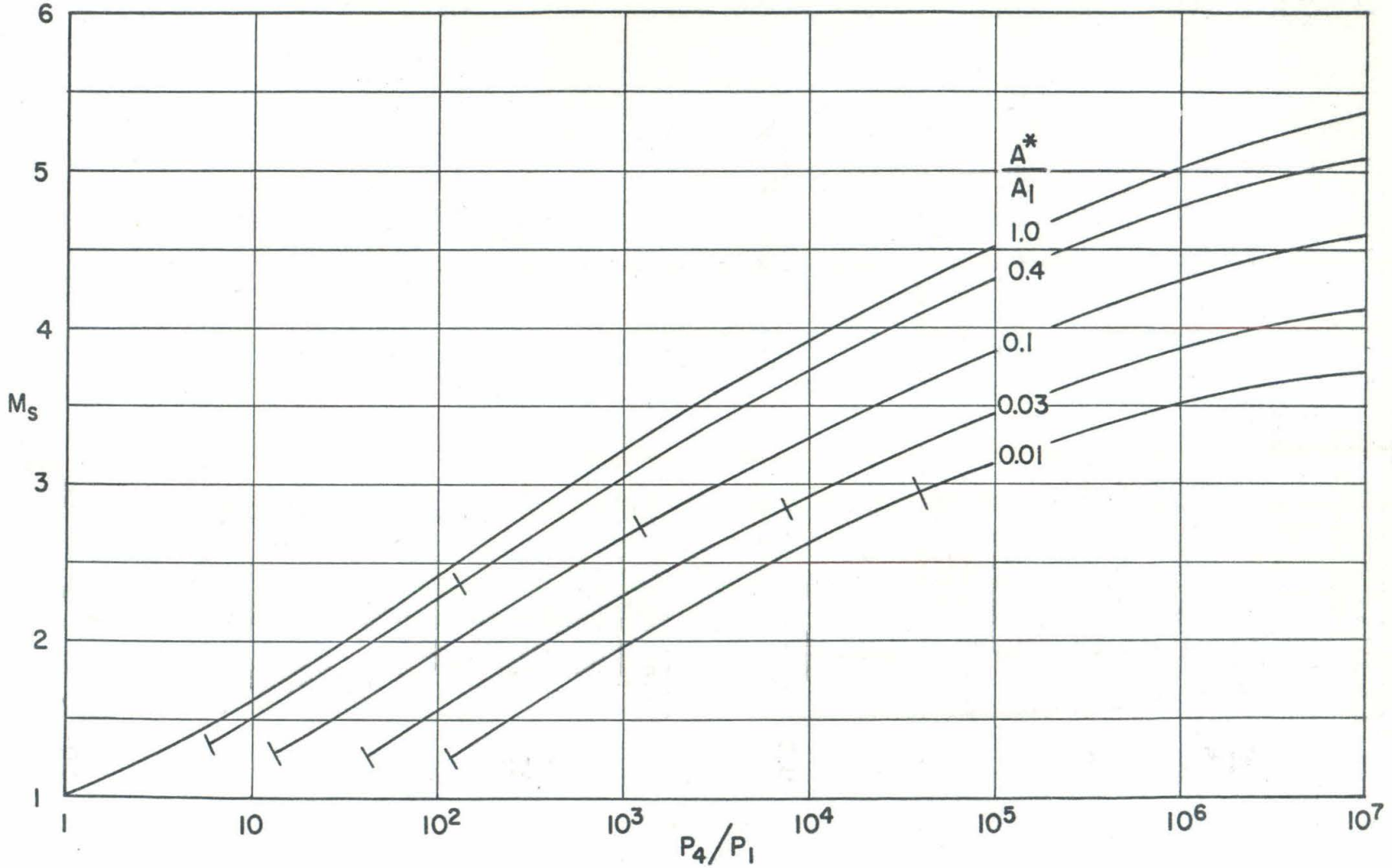

FIG. 3 BASIC PERFORMANCE -- NITROGEN-AIR SHOCK TUBE; $A_4/A_1 = 1$

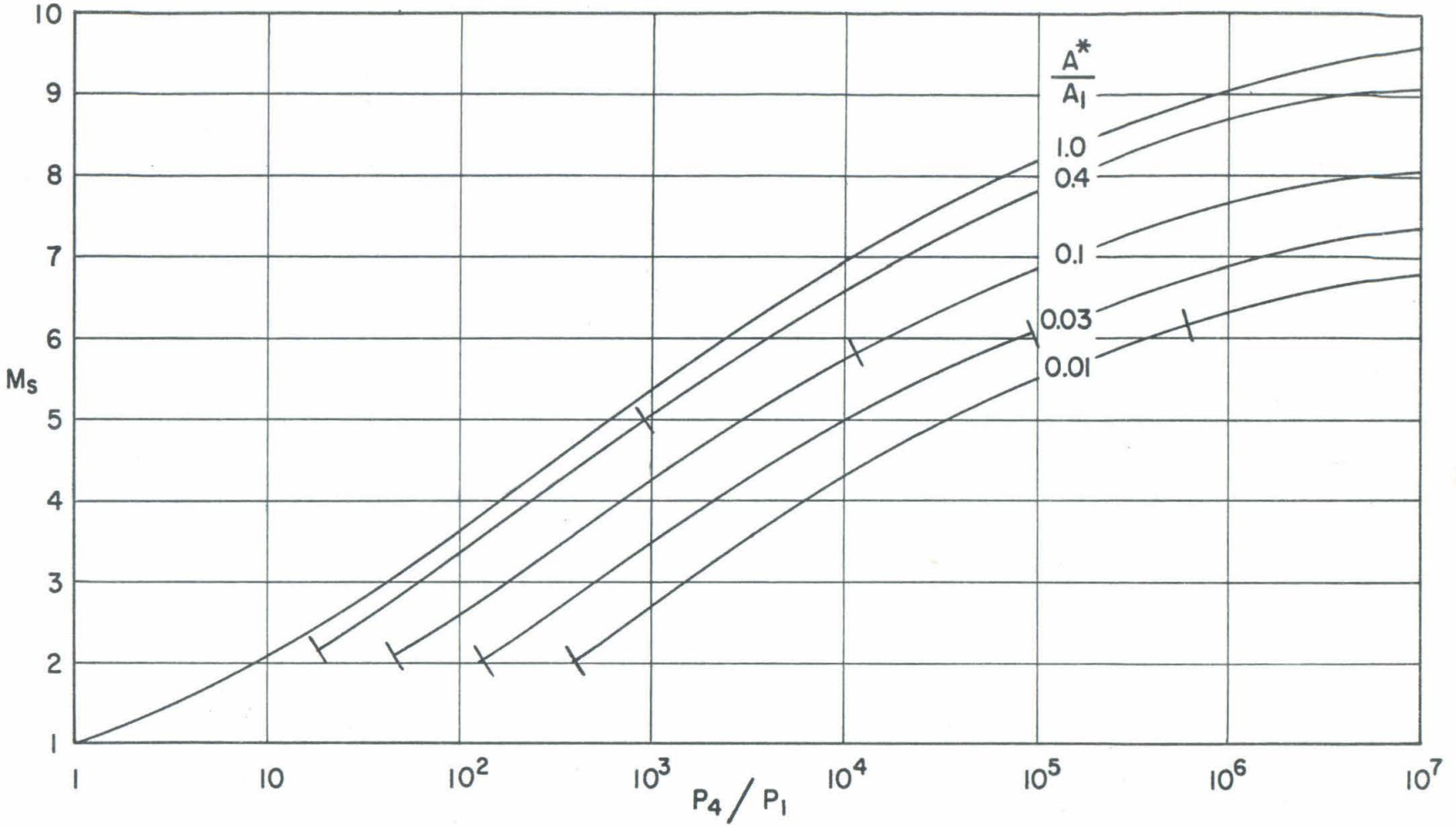

FIG. 4 BASIC PERFORMANCE -- HELIUM-AIR SHOCK TUBE; $A_4/A_1 = 1$

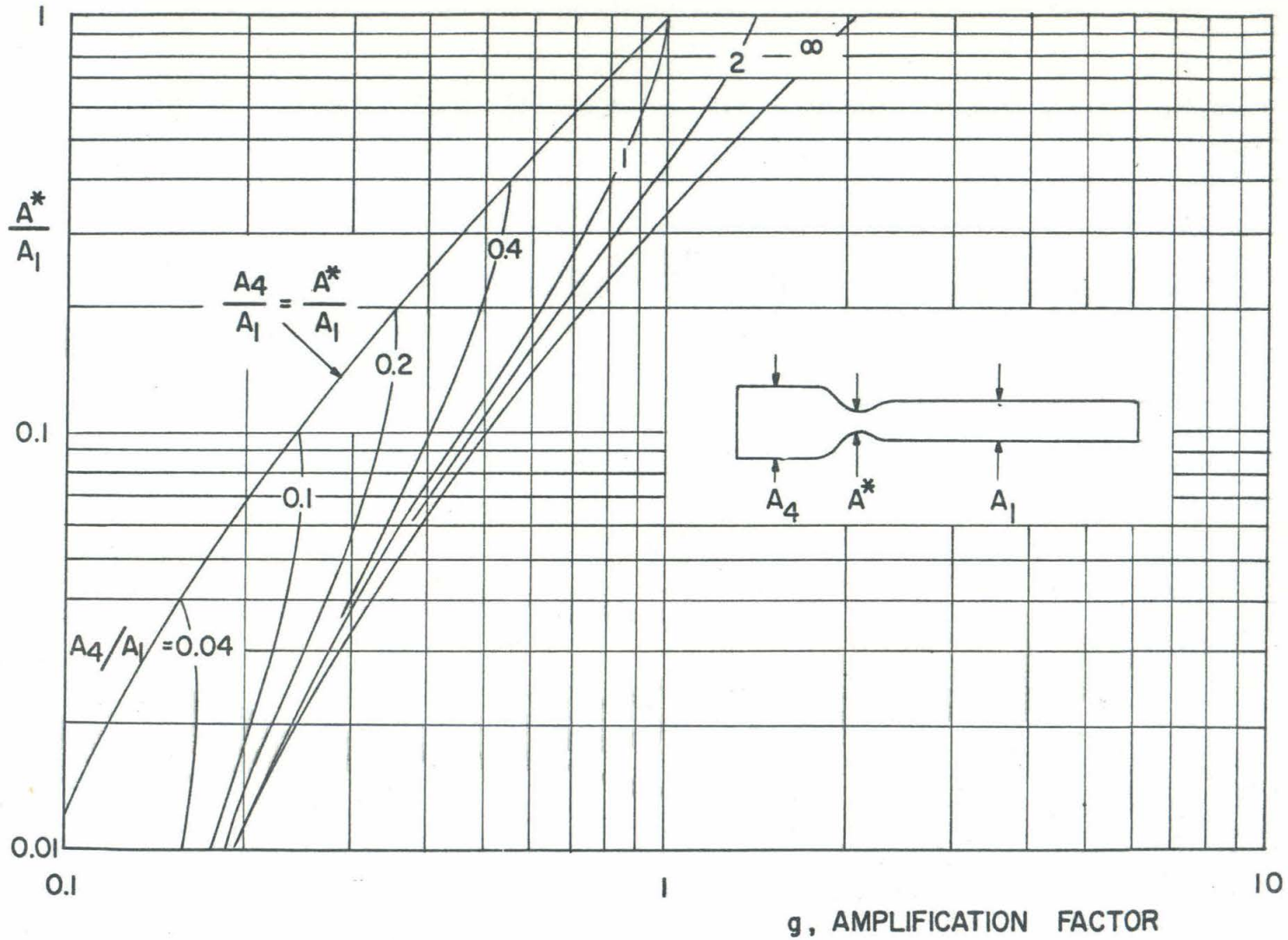

FIG. 5(a) AMPLIFICATION FACTOR FOR $\gamma = 5/3$

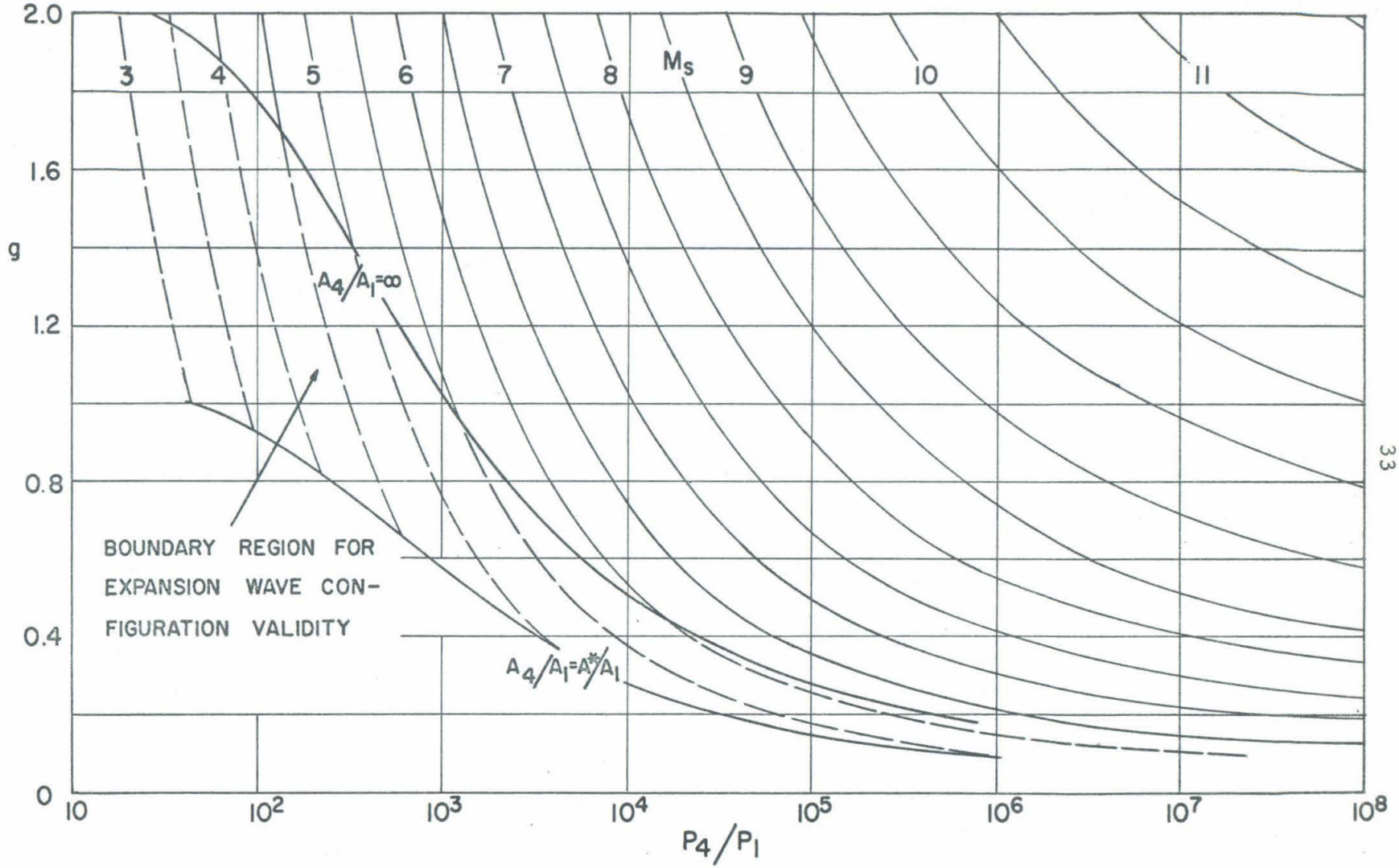

FIG. 5(b) BASIC PERFORMANCE--HELIUM-AIR SHOCK TUBE; EXPANSION WAVE CONFIGURATION

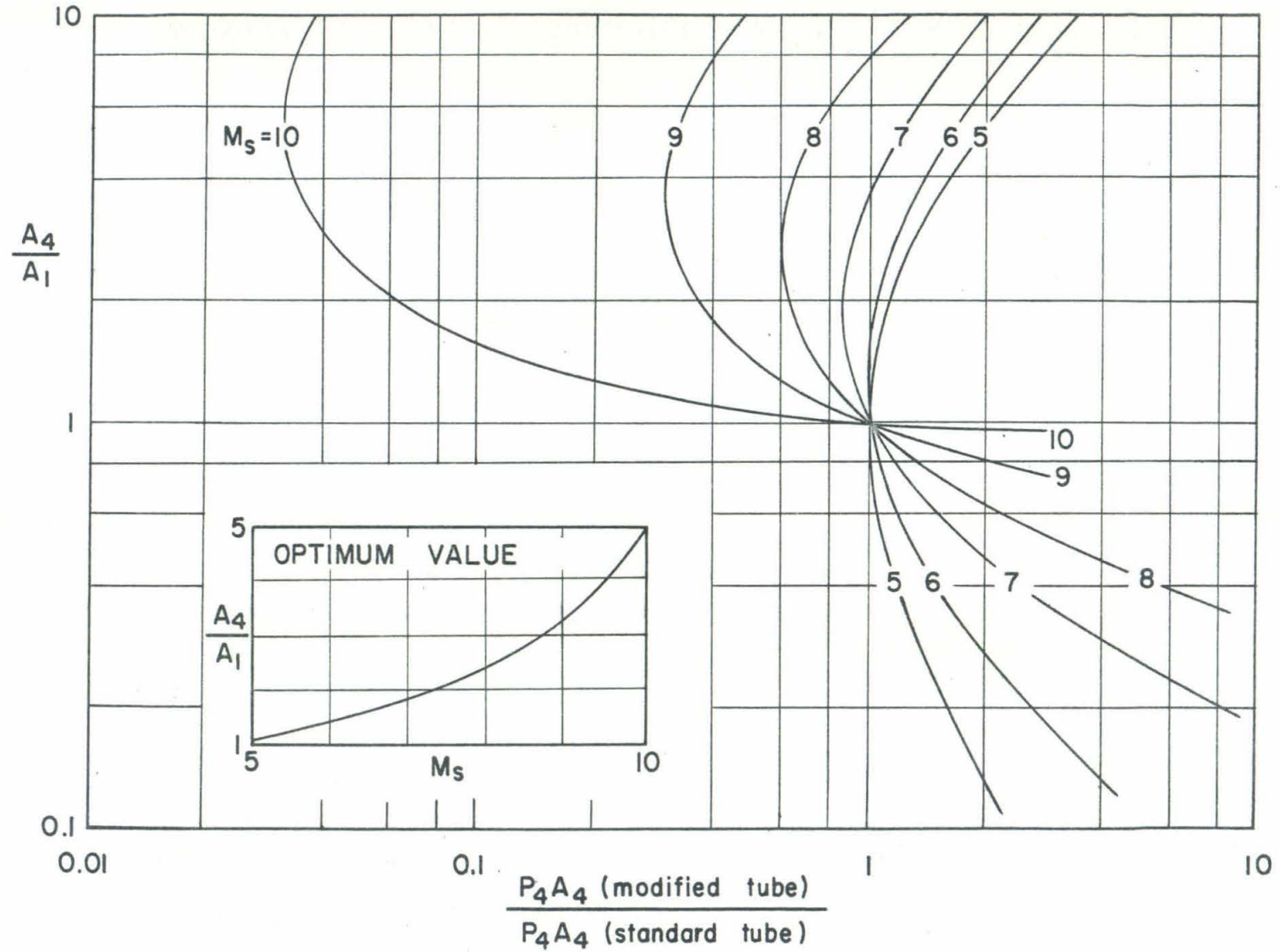

FIG. 6 OPTIMIZATION OF A_4/A_1 FOR ECONOMICAL OPERATION -- HELIUM-AIR SHOCK TUBE

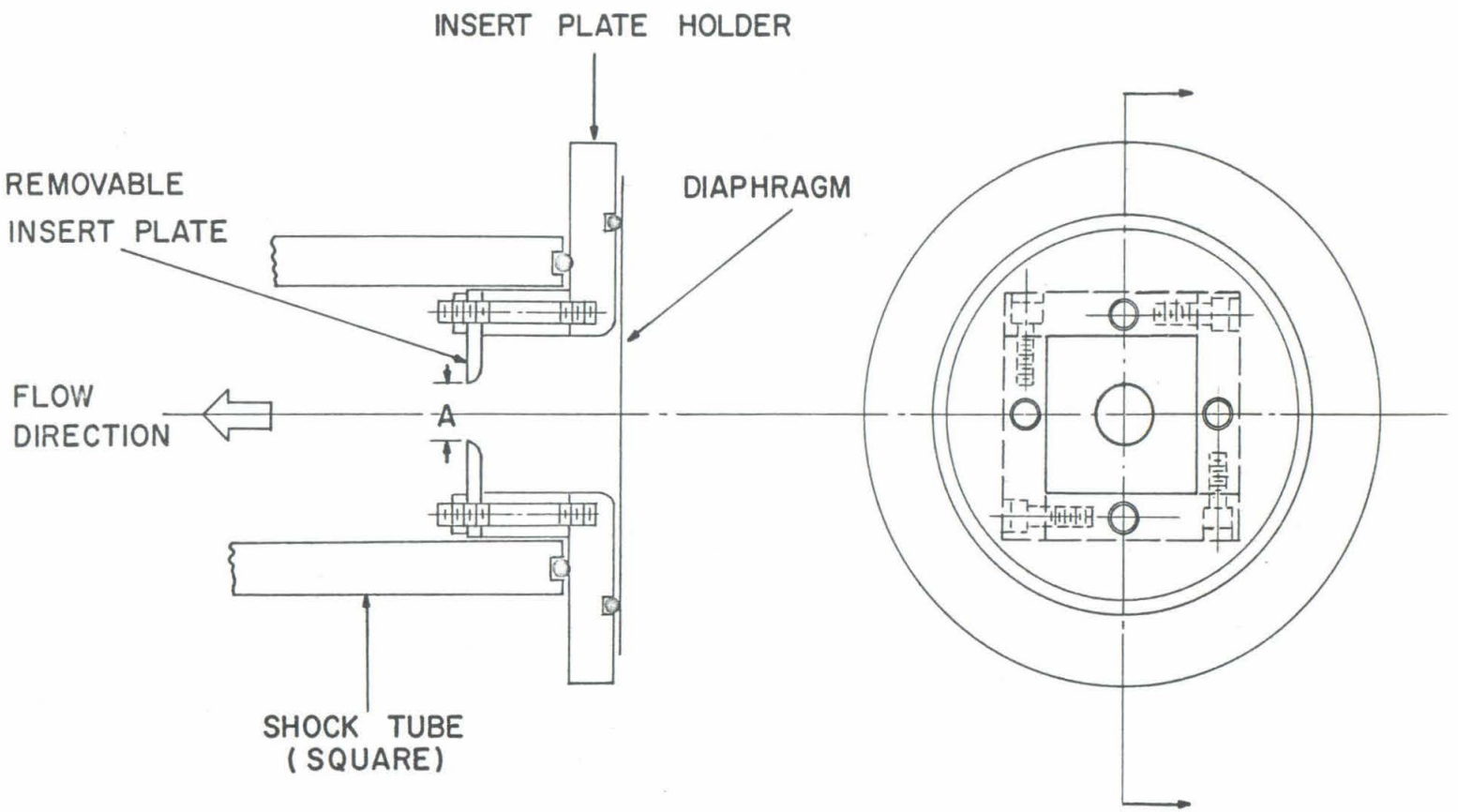

FIG. 7 DIAPHRAGM INSERT SECTION -- 1/2 SCALE

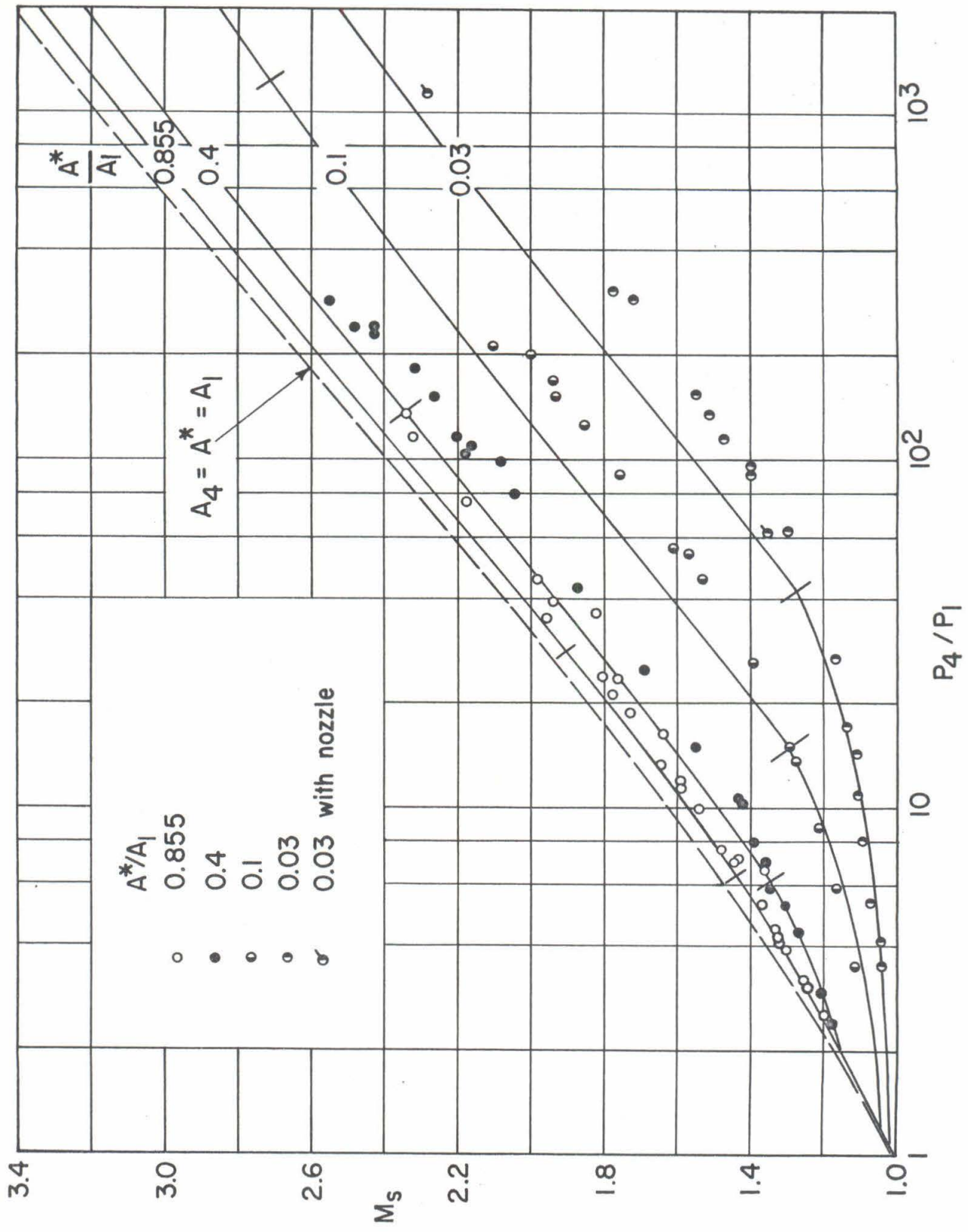

FIG. 8 UNCORRECTED DATA -- NITROGEN-AIR SHOCK TUBE; $A_4/A_1 = 0.855$

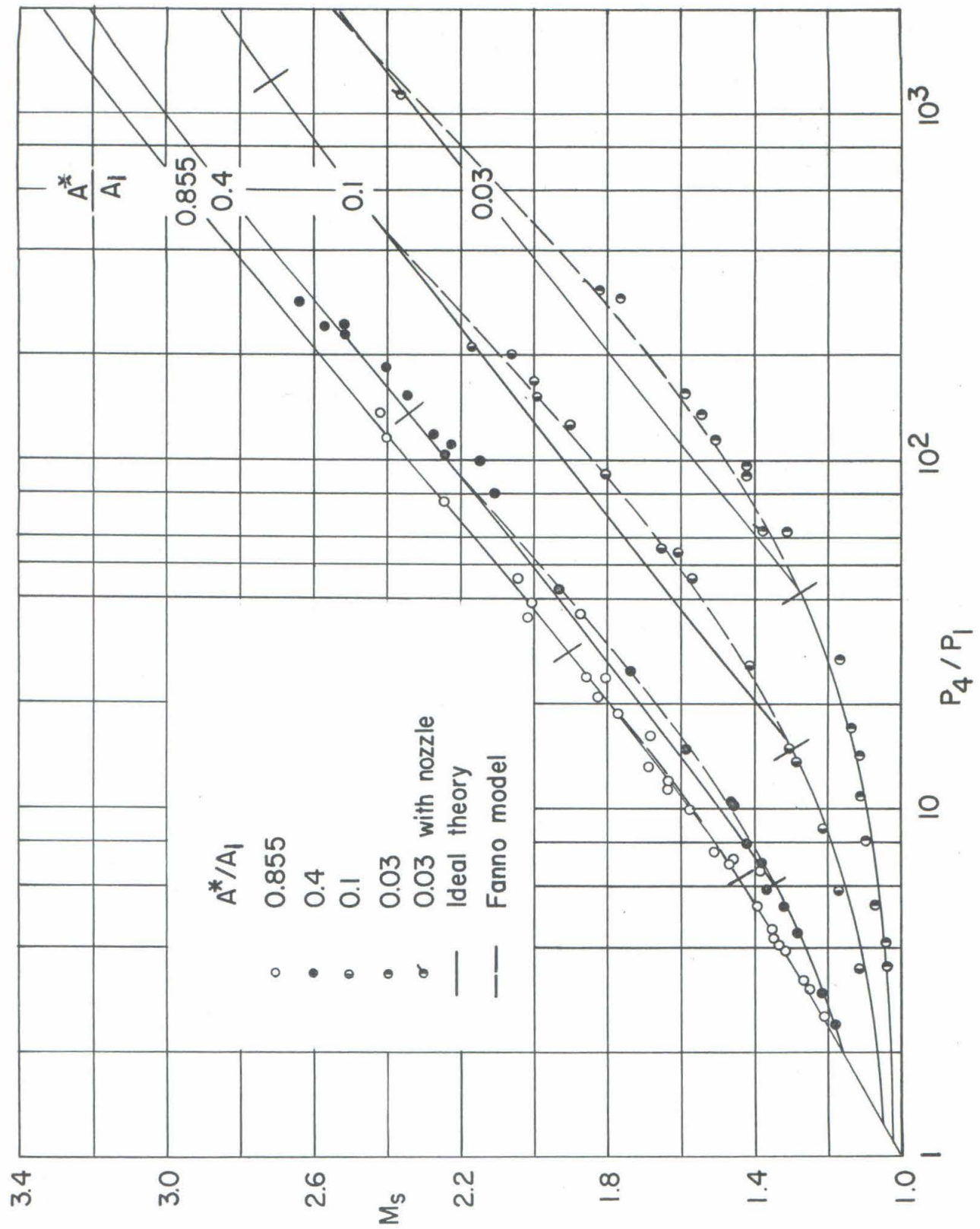

FIG. 9 CORRECTED DATA -- NITROGEN-AIR SHOCK TUBE
$A_4/A_1 = 0.855$

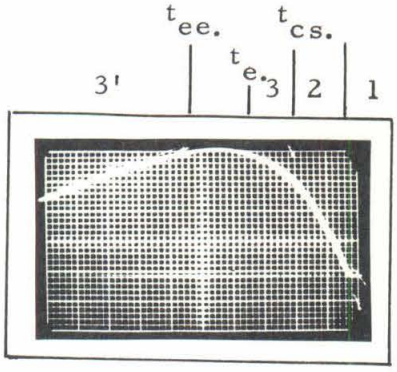

$M_s = 3.16$
$P_1 = 1.0$ mm.
1 mv./div.
1 ms./div.
x = 15.5 ft.

$(s_2/s_{3'})_{exp.} = -6.9$
$(s_2/s_{3'})_{th.} = -7.5$
$(s_2/s_3)_{th.} = +7.5$

31D2

(a) Expansion Wave Configuration; $A^*/A_1 = 0.1$

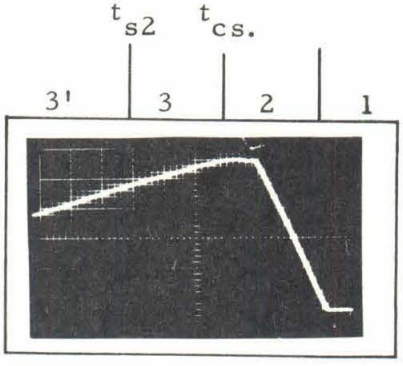

$M_s = 2.22$
$P_1 = 10$ mm.
1 mv./div.
1 ms./div.
x = 15.5 ft.

$(s_2/s_3)_{exp.} = -7.7$
$(s_2/s_3)_{th.} = -2.0$
$(s_2/s_{3'})_{th.} = -7.8$

27D1

(b) Normal Shock Wave Configuration; $A^*/A_1 = 0.1$

FIG. 10 ILLUSTRATIVE FINE WIRE RESPONSE; $1\frac{1}{2}$ MIL. WIRE

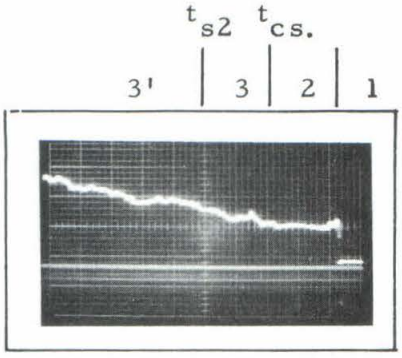

$M_s = 2.11$
$P_1 = 16$ mm.
5 mv./div.
2 ms./div.
x = 17.5 ft.

$(P_2/P_3)_{th.} = 1.0$
$(P_3/P_{3'})_{th.} = 4.2$

5J6

(a) Side Wall Trace; $A^*/A_1 = 0.1$

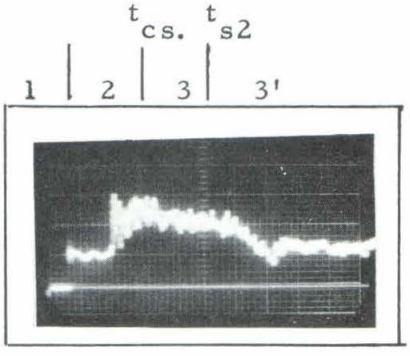

$M_s = 2.06$
$P_1 = 20$ mm.
200 mv./div.
2 ms./div.
x = 17.5 ft.

$(P_{T_{2g}}/P_{T_{3g}})_{th.} = .44$
$(P_{T_{3g}}/P_{T_{3'g}})_{th.} = .75$

3F2

(b) Total Pressure Trace; $A^*/A_1 = 0.1$

FIG. 11 ILLUSTRATIVE PRESSURE TRACES

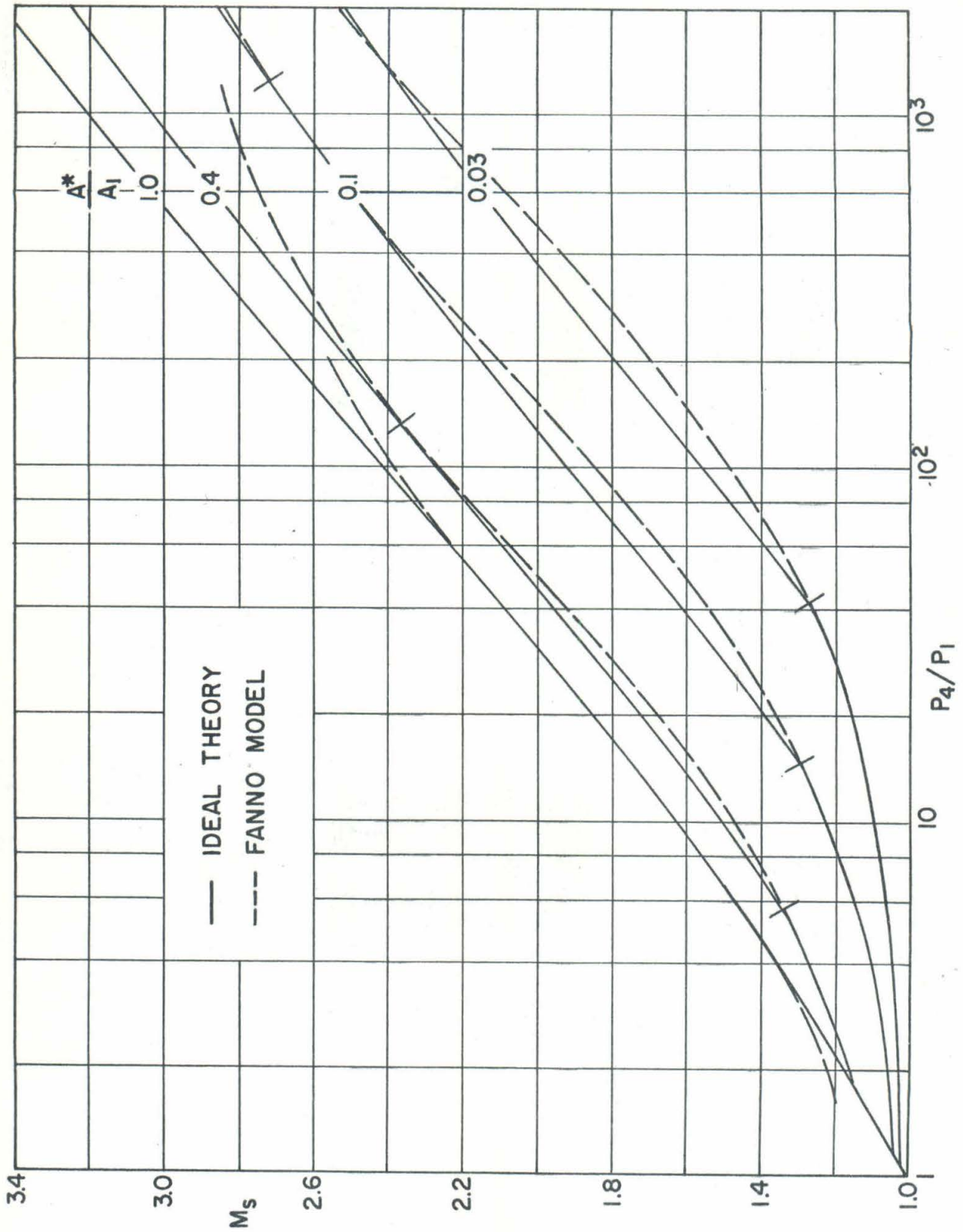

FIG. 12 THE FANNO PROCESS MODEL--NITROGEN-AIR SHOCK TUBE; $A_4/A_1 = 1$

1 February 1960

GUGGENHEIM AERONAUTICAL LABORATORY
CALIFORNIA INSTITUTE OF TECHNOLOGY

HYPERSONIC RESEARCH PROJECT
Contract No. DA-04-495-Ord-19

DISTRIBUTION LIST

U. S. Government Agencies

Los Angeles Ordnance District
55 South Grand Avenue
Pasadena 2, California
Attention: Mr. E. L. Stone
2 copies

Los Angeles Ordnance District
55 South Grand Avenue
Pasadena 2, California
Attention: ORDEV-00-
Mr. Typaldos

Chief of Ordnance
Department of the Army
ORDTB - Ballistic Section
The Pentagon
Washington 25, D. C.
Attention: Mr. G. Stetson

Chief of Ordnance
Department of the Army
Washington 25, D. C.
Attention: ORDTB
For Transmittal To
Department of Commerce
Office of Technical Information

Office of Ordnance Research
Box CM, Duke Station
Durham, North Carolina
10 copies

Ordnance Aerophysics Laboratory
Daingerfield, Texas
Attention: Mr. R. J. Valluz

Commanding Officer
Diamond Ordnance Fuze Laboratories
Washington 25, D. C.
Attention: ORDTL 06.33

Commanding General
Army Ballistics Missile Agency
Huntsville, Alabama
Attention: ORDAB-1P
2 copies

Commanding General
Army Ballistics Missile Agency
Huntsville, Alabama
Attention: ORDAB-DA
Mr. T. G. Reed
3 copies

Commanding General
Redstone Arsenal
Huntsville, Alabama
Attention: Technical Library

Army Ballistic Missile Agency
ORDAB-DA
Development Operations Division
Redstone Arsenal
Huntsville, Alabama
Attention: Dr. Ernst D. Geissler
Director, Aeroballistics Lab.

Army Ballistic Missile Agency
ORDAB-DA
Development Operations Division
Redstone Arsenal
Huntsville, Alabama
Attention: Dr. Daum

Chief of Staff
United States Army
The Pentagon
Washington 25, D. C.
Attention: Director/Research

Exterior Ballistic Laboratories
Aberdeen Proving Ground
Maryland
Attention: Mr. C. L. Poor

Ballsitic Research Laboratories
Aberdeen Proving Ground
Maryland
Attention: Dr. Joseph Sternberg

Commanding General
White Sands Proving Ground
Las Cruces, New Mexico

Commander
Air Force
Office of Scientific Research
Washington 25, D. C.
Attention: RDTRRF

Air Force
Office of Scientific Research
SRR
Washington 25, D. C.
Attention: Dr. Carl Kaplan

Mechanics Division
Air Force
Office of Scientific Research
Washington 25, D. C.

Commander
Hq., Air Research and
Development Command
Bolling Air Force Base
Washington, D. C.
Attention: RDS-TIS-3

Air Force Armament Center
Air Research and Development
Command
Eglin Air Force Base
Florida
Attention: Technical Library

Commander
Wright Air Development Center
Wright-Patterson Air Force Base
Ohio
Attention: WCLSR

Commander
Wright Air Development Center
Wright-Patterson Air Force Base
Ohio
Attention: WCLSW

Commander
Wright Air Development Center
Wright-Patterson Air Force Base
Ohio
Attention: WCOSl-9-5 (Distribution)

Commander
Wright Air Development Center
Wright-Patterson Air Force Base
Ohio
Attention: WCLSW, Mr. P. Antonatos

Commander
Wright Air Development Center
Wright-Patterson Air Force Base
Ohio
Attention: Dr. H. K. Doetsch

Commander
Wright Air Development Center
Wright-Patterson Air Force Base
Ohio
Attention: Dr. G. Guderley

Commander
Wright Air Development Center
Wright-Patterson Air Force Base
Ohio
Attention: WCLJD, Lt. R. D. Stewart

Director of Research and Development
DCS/D
Headquarters
USAF
Washington 25, D. C.
Attention: AFDRD-RE

Commander
Western Development Division
P. O. Box 262
Inglewood, California

Commander
Western Development Division
5760 Arbor Vitae Street
Los Angeles, California
Attention: Maj. Gen. B. A. Schriever

Commander
Arnold Engineering Development Center
Tullahoma, Tennessee
Attention: AEORL

Air University Library
Maxwell Air Force Base
Alabama

Commander
Air Force Missile Development Center
Holloman Air Force Base
New Mexico
Attention: Dr. G. Eber (MDGRS)

U. S. Naval Ordnance Laboratory
White Oak
Silver Spring, Maryland
Attention: Dr. H. Kurzweg

U. S. Naval Ordnance Laboratory
White Oak
Silver Spring 19, Maryland
Attention: Dr. R. K. Lobb

U. S. Naval Ordnance Laboratory
White Oak
Silver Spring 19, Maryland
Attention: Dr. Z. I. Slawsky

U. S. Naval Ordnance Laboratory
White Oak
Silver Spring 19, Maryland
Attention: Dr. R. Wilson

U. S. Naval Ordnance Test Station
China Lake
Inyokern, California
Attention: Mr. Howard R. Kelly, Head
Aerodynamics Branch,
Code 5032

Navy Department
Bureau of Ordnance
Technical Library
Washington 25, D. C.
Attention: Ad-3

Director
Naval Research Laboratory
Washington 25, D. C.

Office of Naval Research
Department of the Navy
Washington 25, D. C.
Attention: Mr. M. Tulin

Commander
U. S. Naval Proving Ground
Dahlgren, Virginia

Bureau of Aeronautics
Department of the Navy
Room 2 w 75
Washington 25, D. C.
Attention: Mr. F. A. Louden

Commander
Armed Services Technical Information
Agency
Attention: TIPDR
Arlington Hall Station
Arlington 12, Virginia
10 copies

National Bureau of Standards
Department of Commerce
Washington 25, D. C.
Attention: Dr. G. B. Schubauer

National Aeronautics and Space
Administration
1512 H Street, N. W.
Washington 25, D. C.
Attention: Dr. H. L. Dryden, Director
5 copies

National Aeronautics and Space
Administration
Ames Aeronautical Laboratory
Moffett Field, California
Attention: Mr. H. Julian Allen

National Aeronautics and Space
Administration
Ames Aeronautical Laboratory
Moffett Field, California
Attention: Dr. D. Chapman

National Aeronautics and Space
Administration
Ames Aeronautical Laboratory
Moffett Field, California
Attention: Dr. A. C. Charters

National Aeronautics and Space
Administration
Ames Aeronautical Laboratory
Moffett Field, California
Attention: Mr. A. J. Eggers

National Aeronautics and Space
Administration
Ames Aeronautical Laboratory
Moffett Field, California
Attention: Mr. Robert T. Jones

National Aeronautics and Space
Administration
Ames Aeronautical Laboratory
Moffett Field, California
Attention: Dr. M. K. Rubesin

National Aeronautics and Space
Administration
Ames Aeronautical Laboratory
Moffett Field, California
Attention: Mr. J. R. Stalder

National Aeronautics and Space
Administration
Langley Aeronautical Laboratory
Langley Field, Virginia
Attention: Mr. M. Bertram

National Aeronautics and Space
Administration
Langely Aeronautical Laboratory
Langley Field, Virginia
Attention: Dr. A. Busemann

National Aeronautics and Space
Administration
Langely Aeronautical Laboratory
Langley Field, Virginia
Attention: Mr. Clinton E. Brown

National Aeronautics and Space
Administration
Langley Aeronautical Laboratory
Langley Field, Virginia
Attention: Mr. C. McLellan

National Aeronautics and Space
Administration
Langley Aeronautical Laboratory
Langley Field, Virginia
Attention: Mr. John Stack

National Aeronautics and Space
Administration
Lewis Research Center
21000 Brookpark Road
Cleveland 35, Ohio
Attention: Library
George Mandel
2 copies

Technical Information Service
P. O. Box 62
Oak Ridge, Tennessee

U. S. Government Agencies
For Transmittal to
Foreign Countries

Chief of Ordnance
Department of the Army
Washington 25, D. C.
Attention: ORDGU-SE
Foreign Relations Section
For Transmittal To
Australian Joint Services Mission

Chief of Ordnance
Department of the Army
Washington 25, D. C.
Attention: ORDGU-SE
Foreign Relations Section
For Transmittal To
Canadian Joint Staff

Chief of Ordnance
Department of the Army
Washington 25, D. C.
Attention: ORDGU-SE
Foreign Relations Section
For Transmittal To
Professor S. Irmay
Division of Hydraulic Engineering
TECHNION
Israel Institute of Technology
Haifa, Israel

Chief of Ordnance
Department of the Army
Washington 25, D. C.
Attention: ORDGU-SE
Foreign Relations Section
For Transmittal To
Dr. Josef Rabinowicz
Department of Aeronautical Engineering
TECHNION
Israel Institute of Technology
Haifa, Israel

Chief of Ordnance
Department of the Army
Washington 25, D. C.
Attention: ORDGU-SE
Foreign Relations Section
For Transmittal To
Dr. Yosujiro Kobashi
Aerodynamics Division
National Aeronautical Laboratory
Shinkawa 700 Mitaka City
Tokyo, Japan

Chief of Ordnance
Department of the Army
Washington 25, D. C.
Attention: ORDGU-SE
Foreign Relations Section
For Transmittal To
Professor Itiro Tani
Aeronautical Research Institute
Tokyo University
Komaba, Meguro-ku
Toyko, Japan

Chief of Ordnance
Department of the Army
Washington 25, D. C.
Attention: ORDGU-SE
Foreign Relations Section
For Transmittal To
Professor D. C. Pack
Royal Technical College
Glasgow, Scotland

Chief of Ordnance
Department of the Army
Washington 25, D. C.
Attention: ORDGU-SE
Foreign Relations Section
For Transmittal To
The Aeronautical Research
Institute of Sweden
Ulvsunda 1, Sweden
Attention: Mr. Georg Drougge

Commanding Officer
Office of Naval Research
Branch Office
Navy, 100
FPO
New York, N. Y.
2 copies

Air Research and Development Command
European Office
Shell Building
60 Rue Rabenstein
Brussels, Belgium
Attention: Col. Lee Gossick, Chief
5 copies

Centre de Formation en Aerodynamique
Experimentale, C. F. A. E.
Rhode-Saint-Genese
72 Chaussee de Waterloo
Belgium
Attention: Library (1 copy)
Attention: Dr. Robert H. Korkegi (1 copy)

Universities and Non-Profit Organizations

Brown University
Providence 12, Rhode Island
Attention: Professor R. Meyer

Brown University
Graduate Division of Applied Mathematics
Providence 12, Rhode Island
Attention: Dr. W. Prager

Brown University
Graduate Division of Applied Mathematics
Providence 12, Rhode Island
Attention: Dr. R. Probstein

University of California
Low Pressures Research
Institute of Engineering Research
Engineering Field Station
1301 South 46th Street
Richmond, California
Attention: Professor S. A. Schaaf

University of California at Los Angeles
Department of Engineering
Los Angeles 24, California
Attention: Dr. L. M. K. Boelter

University of California at Los Angeles
Department of Engineering
Los Angeles 24, California
Attention: Professor J. Miles

Case Institute of Technology
Cleveland, Ohio
Attention: Dr. G. Kuerti

Catholic University of America
Department of Physics
Washington 17, D. C.
Attention: Professor K. F. Herzfeld

Cornell University
Graduate School of Aeronautical Engineering
Ithaca, New York
Attention: Dr. E. L. Resler, Jr.

Cornell University
Graduate School of Aeronautical Engineering
Ithaca, New York
Attention: Dr. W. R. Sears

Cornell University
College of Engineering
Ithaca, New York
Attention: Professor N. Rott

University of Florida
Department of Aeronautical Engineering
Gainesville, Florida
Attention: Professor D. T. Williams

Harvard University
Department of Applied Physics and
Engineering Science
Cambridge 38, Massachusetts
Attention: Dr. A. Bryson

Harvard University
Department of Applied Physics and
Engineering Science
Cambridge 38, Massachusetts
Attention: Dr. H. W. Emmons

University of Illinois
Department of Aeronautical Engineering
Urbana, Illinois
Attention: Dr. Allen I. Ormsbee

University of Illinois
Aeronautical Institute
Urbana, Illinois
Attention: Professor H. O. Barthel

The Johns Hopkins University
Applied Physics Laboratory
8621 Georgia Avenue
Silver Spring, Maryland
Attention: Dr. E. A. Bonney

The Johns Hopkins University
Applied Physics Laboratory
8621 Georgia Avenue
Silver Spring, Maryland
Attention: Dr. F. N. Frenkiel

The Johns Hopkins University
Applied Physics Laboratory
8621 Georgia Avenue
Silver Spring, Maryland
Attention: Dr. F. K. Hill

The Johns Hopkins University
Department of Aeronautical Engineering
Baltimore 18, Maryland
Attention: Dr. F. H. Clauser

The Johns Hopkins University
Department of Aeronautical Engineering
Baltimore 18, Maryland
Attention: Dr. L. Kovasznay

The Johns Hopkins University
Department of Mechanical Engineering
Baltimore 18, Maryland
Attention: Dr. S. Corrsin

Lehigh University
Physics Department
Bethlehem, Pennsylvania
Attention: Dr. R. Emrich

Los Alamos Scientific Laboratory
of the University of California
J Division
P. O. Box 1663
Los Alamos, New Mexico
Attention: Dr. Keith Boyer

University of Maryland
Department of Aeronautical Engineering
College Park, Maryland
Attention: Dr. S. F. Shen

University of Maryland
Institute of Fluid Dynamics and
Applied Mathematics
College Park, Maryland
Attention: Director

University of Maryland
Institute of Fluid Dynamics and
Applied Mathematics
College Park, Maryland
Attention: Professor J. M. Burgers

University of Maryland
Institute of Fluid Dynamics and
Applied Mathematics
College Park, Maryland
Attention: Professor F. R. Hama

University of Maryland
Institute of Fluid Dynamics and
Applied Mathematics
College Park, Maryland
Attention: Professor S. I. Pai

Massachusetts Institute of Technology
Cambridge 39, Massachusetts
Attention: Dr. A. H. Shapiro

Massachusetts Institute of Technology
Department of Aeronautical Engineering
Cambridge 39, Massachusetts
Attention: Professor M. Finston

Massachusetts Institute of Technology
Department of Aeronautical Engineering
Cambridge 39, Massachusetts
Attention: Professor E. Mollo-Christensen

Massachusetts Institute of Technology
Department of Aeronautical Engineering
Cambridge 39, Massachusetts
Attention: Dr. G. Stever

Massachusetts Institute of Technology
Fluid Dynamics Research Group
Cambridge 39, Massachusetts
Attention: Dr. Leon Trilling

Massachusetts Institute of Technology
Department of Mathematics
Cambridge 39, Massachusetts
Attention: Professor C. C. Lin

University of Michigan
Ann Arbor, Michigan
Attention: Dr. H. P. Liepmann

University of Michigan
Department of Aeronautical Engineering
Ann Arbor, Michigan
Attention: Dr. Arnold Kuethe

University of Michigan
Department of Aeronautical Engineering
East Engineering Building
Ann Arbor, Michigan
Attention: Professor W. C. Nelson

University of Michigan
Department of Aeronautical Engineering
Aircraft Propulsion Laboratory
Ann Arbor, Michigan
Attention: Mr. J. A. Nicholls

University of Michigan
Department of Aeronautical Engineering
Ann Arbor, Michigan
Attention: Professor W. W. Willmarth

University of Michigan
Department of Physics
Ann Arbor, Michigan
Attention: Dr. O. Laporte

University of Minnesota
Department of Aeronautical Engineering
Minneapolis 14, Minnesota
Attention: Professor J. D. Akerman

University of Minnesota
Department of Aeronautical Engineering
Minneapolis 14, Minnesota
Attention: Dr. C. C. Chang

University of Minnesota
Department of Aeronautical Engineering
Minneapolis 14, Minnesota
Attention: Dr. R. Hermann

University of Minnesota
Department of Mechanical Engineering
Division of Thermodynamics
Minneapolis, Minnesota
Attention: Dr. E. R. G. Eckert

New York University
Department of Aeronautics
University Heights
New York 53, New York
Attention: Dr. J. F. Ludloff

New York University
Institute of Mathematics and Mechanics
45 Fourth Street
New York 53, New York
Attention: Dr. R. W. Courant

North Carolina State College
Department of Engineering
Raleigh, North Carolina
Attention: Professor R. M. Pinkerton

Northwestern University
Gas Dynamics Laboratory
Evanston, Illinois
Attention: Professor A. B. Cambel

Ohio State University
Aeronautical Engineering Department
Columbus, Ohio
Attention: Professor A. Tifford

Ohio State University
Aeronautical Engineering Department
Columbus, Ohio
Attention: Professor G. L. von Eschen

University of Pennsylvania
Philadelphia, Pennsylvania
Attention: Professor M. Lessen

Polytechnic Institute of Brooklyn
Aerodynamic Laboratory
527 Atlantic Avenue
Freeport, New York
Attention: Dr. A. Ferri

Polytechnic Institute of Brooklyn
Aerodynamic Laboratory
527 Atlantic Avenue
Freeport, New York
Attention: Dr. P. Libby

Polytechnic Institute of Brooklyn
527 Atlantic Avenue
Freeport, New York
Attention: Library

Princeton University
Forrestal Research Center
Princeton, New Jersey
Attention: Library

Princeton University
Aeronautics Department
Forrestal Research Center
Princeton, New Jersey
Attention: Professor S. Bogdonoff

Princeton University
Forrestal Research Center
Building D
Princeton, New Jersey
Attention: Dr. Sin-I Cheng

Princeton University
Aeronautics Department
Forrestal Research Center
Princeton, New Jersey
Attention: Dr. L. Crocco

Princeton University
Aeronautics Department
Forrestal Research Center
Princeton, New Jersey
Attention: Professor Wallace Hayes

Princeton University
Palmer Physical Laboratory
Princeton, New Jersey
Attention: Dr. W. Bleakney

Purdue University
School of Aeronautical Engineering
Lafayette, Indiana
Attention: Librarian

Purdue University
School of Aeronautical Engineering
Lafayette, Indiana
Attention: Professor H. DeGroff

Rensselaer Polytechnic Institute
Aeronautics Department
Troy, New York
Attention: Dr. R. P. Harrington

Rensselaer Polytechnic Institute
Aeronautics Department
Troy, New York
Attention: Dr. T. Y. Li

Rouss Physical Laboratory
University of Virginia
Charlottesville, Virginia
Attention: Dr. J. W. Beams

University of Southern California
Engineering Center
3518 University Avenue
Los Angeles 7, California
Attention: Dr. Raymond Chuan

University of Southern California
Aeronautical Laboratories Department
Box 1001
Oxnard, California
Attention: Mr. J. H. Carrington,
Chief Engineer

Stanford University
Department of Mechanical Engineering
Palo Alto, California
Attention: Dr. D. Bershader

Stanford University
Department of Aeronautical Engineering
Palo Alto, California
Attention: Professor Walter Vincenti

University of Texas
Defense Research Laboratory
500 East 24th Street
Austin, Texas
Attention: Professor M. J. Thompson

University of Washington
Department of Aeronautical Engineering
Seattle 5, W shington
Attention: Professor F. S. Eastman

University of Washington
Department of Aeronautical Engineering
Seattle 5, Washington
Attention: Professor R. E. Street

University of Wisconsin
Department of Chemistry
Madison, Wisconsin
Attention: Dr. J. O. Hirschfelder

Institute of the Aeronautical Sciences
2 East 64th Street
New York 21, New York
Attention: Library

National Science Foundation
Washington 25, D. C.
Attention: Dr. J. McMillan

National Science Foundation
Washington 25, D. C.
Attention: Dr. R. Seeger

Industrial Companies and Research Companies

Aeronautical Research Associates
of Princeton
50 Washington Road
Princeton, New Jersey
Attention: Dr. Coleman Du P. Donaldson

Aeronutronic Systems, Inc.
1234 Air Way
Glendale, California
Attention: Dr. J. Charyk

Aeronutronic Systems, Inc.
1234 Air Way
Glendale, California
Attention: Dr. L. Kavanau

Aerophysics Development Corp.
P. O. Box 689
Santa Barbara, California
Attention: Librarian

Allied Research Associates, Inc.
43 Leon Street
Boston, Massachusetts
Attention: Dr. T. R. Goodman

ARO, Inc.
P. O. Box 162
Tullahoma, Tennessee
Attention: Dr. B. Goethert

ARO, Inc.
G. D. F.
Arnold Air Force Station
Tennessee
Attention: J. L. Potter

ARO, Inc.
P. O. Box 162
Tullahoma, Tennessee
Attention: Librarian,
Gas Dynamics Facility

AVCO Manufacturing Corp.
2385 Revere Beach Parkway
Everett 49, Massachusetts
Attention: Dr. A. Kantrowitz

AVCO Manufacturing Corp.
2385 Revere Beach Parkway
Everett 49, Massachusetts
Attention: Dr. Harry E. Petschek

AVCO Manufacturing Corp.
Advanced Development Division
2385 Revere Beach Parkway
Everett 49, Massachusetts
Attention: Dr. F. R. Riddell

AVCO Manufacturing Corp.
2385 Revere Beach Parkway
Everett 49, Massachusetts
Attention: Library

Boeing Airplane Company
P. O. Box 3107
Seattle 14, Washington
Attention: Mr. G. Snyder

Chance Vought Aircraft, Inc.
P. O. Box 5907
Dallas, Texas
Attention: Mr. J. R. Clark

CONVAIR
A Division of General Dynamics Corp.
San Diego 12, California
Attention: Mr. C. Bossart

CONVAIR
A Division of General Dynamics Corp.
San Diego 12, California
Attention: Mr. W. H. Dorrance
Dept. 1-16

CONVAIR
A Division of General Dynamics Corp.
San Diego 12, California
Attention: Mr. W. B. Mitchell

CONVAIR
A Division of General Dynamics Corp.
Scientific Research Laboratory
5001 Kearny Villa Road
San Diego 11, California
Attention: Mr. Merwin Sibulkin

CONVAIR
A Division of General Dynamics Corp.
Fort Worth 1, Texas
Attention: Mr. W. B. Fallis

CONVAIR
A Division of General Dynamics Corp.
Fort Worth 1, Texas
Attention: Mr. E. B. Maske

CONVAIR
A Division of General Dynamics Corp.
Fort Worth 1, Texas
Attention: Mr. W. G. McMullen

CONVAIR
A Division of General Dynamics Corp.
Fort Worth 1, Texas
Attention: Mr. R. H. Widmer

Cooperative Wind Tunnel
950 South Raymond Avenue
Pasadena, California
Attention: Mr. F. Felberg

Cornell Aeronautical Laboratory
Buffalo, New York
Attention: Dr. A. Flax

Cornell Aeronautical Laboratory
Buffalo, New York
Attention: Mr. A. Hertzberg

Cornell Aeronautical Laboratory
Buffalo, New York
Attention: Dr. F. K. Moore

Douglas Aircraft Company
Santa Monica, California
Attention: Mr. J. Gunkel

Douglas Aircraft Company
Santa Monica, California
Attention: Mr. Ellis Lapin

Douglas Aircraft Company
Santa Monica, California
Attention: Mr. H. Luskin

Douglas Aircraft Company
Santa Monica, California
Attention: Dr. W. B. Oswald

Douglas Aircraft Company
El Segundo Division
827 Lapham Street
El Segundo, California
Attention: Dr. A. M. O. Smith

General Electric Company
Research Laboratory
Schenectady, New York
Attention: Dr. H. T. Nagamatsu

General Electric Company
Missile and Ordnance Systems Department
3198 Chestnut Street
Philadelphia 4, Pennsylvania
Attention: Documents Library,
L. Chasen, Mgr. Libraries

General Electric Company
Aeroscience Laboratory - MSVD
3750 "D" Street
Philadelphia 24, Pennsylvania
Attention: Library

Giannini Controls Corporation
918 East Green Street
Pasadena, California
Attention: Library

The Glenn L. Martin Company
Aerophysics Research Staff
Flight Vehicle Division
Baltimore 3, Maryland
Attention: Dr. Mark V. Morkovin

The Glenn L. Martin Company
Baltimore 3, Maryland
Attention: Mr. G. S. Trimble, Jr.

Grumman Aircraft Engineering Corp.
Bethpage, New York
Attention: Mr. C. Tilgner, Jr.

Hughes Aircraft Company
Culver City, California
Attention: Dr. A. E. Puckett

Lockheed Aircraft Corporation
Missiles Division
Van Nuys, California
Attention: Library

Lockheed Missile Systems Division
Research and Development Laboratory
Sunnyvale, California
Attention: Dr. W. Griffith

Lockheed Missile Systems Division
P. O. Box 504
Sunnyvale, California
Attention: Dr. L. H. Wilson

Lockheed Missile Systems Division
Lockheed Aircraft Corporation
Palo Alto, California
Attention: Mr. R. Smelt

Lockheed Missile Systems Division
Lockheed Aircraft Corporation
Palo Alto, California
Attention: Mr. Maurice Tucker

Marquhardt Aircraft Company
P. O. Box 2013 - South Annex
Van Nuys, California
Attention: Mr. E. T. Pitkin

McDonnell Aircraft Corporation
Lambert - St. Louis Municipal Airport
P. O. Box 516
St. Louis 3, Missouri
Attention: Mr. K. Perkins

Midwest Research Institute
4049 Pennsylvania
Kansas City, Missouri
Attention: Mr. M. Goland, Director
for Engineering Sciences

North American Aviation, Inc.
Aeronautical Laboratory
Downey, California
Attention: Dr. E. R. van Driest

Ramo-Wooldridge Corporation
409 East Manchester Blvd.
Inglewood, California
Attention: Dr. M. U. Clauser

Ramo-Wooldridge Corporation
409 East Manchester Blvd.
Inglewood, California
Attention: Dr. Louis G. Dunn

Ramo-Wooldridge Corporation
P. O. Box 45564, Airport Station
Los Angeles 45, California
Attention: Dr. C. B. Cohen

Ramo-Wooldridge Corporation
P. O. Box 45564, Airport Station
Los Angeles 45, California
Attention: Dr. John Sellars

The RAND Corporation
1700 Main Street
Santa Monica, California
Attention: Library

The RAND Corporation
1700 Main Street
Santa Monica, California
Attention: Dr. C. Gazley

The RAND Corporation
1700 Main Street
Santa Monica, California
Attention: Mr. E. P. Williams

Republic Aviation Corporation
Conklin Street
Farmingdale, Long Island, New York
Attention: Dr. W. J. O'Donnell

Republic Aviation Corporation
Re-Entry Simulation Laboratory
Farmingdale, Long Island, New York

Space Technology Laboratories
P. O. Box 95001
Los Angeles 45, California
Attention: Dr. James E. Broadwell

Space Technology Laboratories
5740 Arbor Vitae
Los Angeles 45, California
Attention: Dr. J. Logan

United Aircraft Corporation
East Hartfort, Connecticut
Attention: Mr. J. G. Lee

Internal

Dr. Harry Ashkenas
Dr. James M. Kendall
Dr. John Laufer
Dr. Thomas Vrebalovich
Dr. Peter P. Wegener
Dr. Harry E. Williams
Mr. Richard Wood
Hypersonic WT; Attn: Mr. G. Goranson
Reports Group
Jet Propulsion Laboratory
4800 Oak Grove Drive
Pasadena 2, California

Dr. S. S. Penner
Dr. Edward Zukoski
Mechanical Engineering Department
California Institute of Technology

Dr. W. D. Rannie
Jet Propulsion Center
California Institute of Technology

Dr. Julian D. Cole
Dr. Donald E. Coles
Dr. P. A. Lagerstrom
Prof. Lester Lees
Dr. H. W. Liepmann
Dr. Clark B. Millikan
Dr. Anatol Roshko

Aeronautics Library
Hypersonic Files (3)
Hypersonic Staff and Research Workers (20)

Foreign

via AGARD Distribution Centers